ELECTRICAL CONDUCTIVITY INHOMOGENEITIES IN THE EARTH'S UPPER MANTLE

by

ROY DAVID HYNDMAN
B.A.Sc., University of British Columbia, 1962

A THESIS SUBMITTED IN PARTIAL FULFILMENT OF
THE REQUIREMENTS FOR THE DEGREE OF
MASTER OF APPLIED SCIENCE

in the Department
of
PHYSICS

We accept this thesis as conforming to the
required standard

THE UNIVERSITY OF BRITISH COLUMBIA
November, 1963

In presenting this thesis in partial fulfilment of the requirements for an advanced degree at the University of British Columbia, I agree that the Library shall make it freely available for reference and study. I further agree that permission for extensive copying of this thesis for scholarly purposes may be granted by the Head of my Department or by his representatives. It is understood that copying or publication of this thesis for financial gain shall not be allowed without my written permission.

Department of PHYSICS

The University of British Columbia,
Vancouver 8, Canada.

Date MARCH 4 1964

ABSTRACT

This study was undertaken in order to investigate the possible occurrence of horizontal variations in the electrical conductivity of the Earth's upper mantle in southwestern Canada, using a series of simultaneous magnetic variograph recordings. Until recently no variation in the conductivity in a horizontal direction had been anticipated nor observed. During the past five years Parkinson in Australia, Rikitake in Japan, Schmucker in Germany and others have observed marked differences in the magnetograms at closely spaced stations. Secondary magnetic fields produced by induction in high conductivity regions in the Earth's upper mantle have been suggested as the cause of these differences.

The profile described in this thesis indicates conductivity inhomogeneities in southwestern British Columbia and southwestern Alberta. The vertical magnetic fields produced by induction in these inhomogeneities for magnetic variations with periods from 10 to 120 minutes have magnitudes of about 30 to 60 percent of the normal horizontal component. The normal vertical component is about 20 percent of the horizontal. These regions appear to be essentially two dimensional with anomalous induction resulting only from that component of the incident magnetic variations which is perpendicular to their strike. This strike and the intensity of the

induced field have been estimated at each station. A pronounced difference has also been found between the vertical component of the diurnal geomagnetic variations at a station in the Rocky Mountains and those at the rest of the stations along the profile.

ACKNOWLEDGEMENTS

Much of the work and results of this thesis must be accredited to the many people who have provided the author with assistance and counsel, in particular, Professor J. A. Jacobs who supervised the research and Mr. J. Martin who assisted throughout the field program. Others who have given major aid are Dr. T. Watanabe who provided many helpful theoretical discussions, Mr. B. Caner of the Victoria Magnetic Observatory who provided valuable assistance in dealing with the problems encountered in making magnetic observations, the faculty and graduate students of the Institute of Earth Sciences at the University of British Columbia and Dr. K. Vozoff of the University of Alberta.

TABLE OF CONTENTS

TABLE OF CONTENTS (continued)

FIGURES

TABLES

APPENDICES

I. INTRODUCTION

As a part of the Canadian Upper Mantle Project a series of geomagnetic variograph stations was set up along a profile extending across southern British Columbia and Alberta in order to investigate the occurrence of any horizontal variations in the electrical conductivity of the Earth's upper mantle.

Detailed analyses by Niblett et al[12], Cantwell[2], Garland and Webster[7] and others using the magnetotelluric method and by Chapman[3] and Rikitake using a spherical harmonic analysis of world wide magnetic variations have outlined the vertical distribution of conductivity assuming a horizontally layered Earth. In particular they have found a sharp discontinuity at a depth of the order of 100 kilometers. Recent studies using closely spaced variograph stations have shown, that in addition to this vertical variation, there are marked conductivity variations in the horizontal direction at some locations. The cause of these variations is an open question, but since electrical conductivity may be related to temperature (Tozer[25]), irregularities in the temperature and heat flow distribution in the upper mantle have been frequently suggested. In particular Rikitake[18] has postulated the existence of high temperature magma pockets. Schmucker[21] has also suggested that there may be irregularities or local deformations of the 100 kilometer discontinuity noted above. This explanation in turn has been given as evidence for the existence of convection cells in the mantle.

Numerous strong localized zones of high electrical conductivity have been found throughout the world. The main evidence for the existence of these regions is a large spatial change in the vertical magnetic component, which for a horizontally stratified Earth should be small at all locations. Rikitake[16][17][19] has described the very large changes in the geomagnetic field variations that occur across Japan and has suggested as an explanation, a rather complicated conductivity configuration. This involves a highly conducting loop rising from depth on either side and extending across the island, and, in order to obtain sufficient induced current intensity, underlain by a low conductivity wedge.

In north Germany, Schmucker[21] has found a narrow region of apparent high conductivity. He has shown that the observed anomaly in magnetic variations cannot be explained in terms of inhomogeneities in the sedimentary layer or deeper inhomogeneities reflected by gravity surveys, and suggests that they are caused by an irregular temperature distribution in the Earth's upper mantle. More recently he has investigated a similar but more complex anomaly in the southwestern United States[22]. Part of the anomaly lies at the Pacific coast, and may be caused by the influence of the land-sea contact. The large vertical components of magnetic disturbances which appear in Australia have been attributed to such a contact by Parkinson[13].

Another interesting example presented by Whitham and

Anderson[32], involves a high conductivity zone lying between Ellesmere Island in northern Canada and Greenland. They have evaluated the parameters for a cylinder model and, although the data are limited, have obtained satisfactory results.

Wiese[33] has used a least squares determination of the correlation between the horizontal and vertical magnetic field variations at a number of stations to determine the strike of conductivity anisotropies that exist in a large area in East Germany.

The magnetotelluric method (Cagniard[1], Price[14] and Wait[28]) in which the ratio of orthogonal horizontal components of the electric and magnetic fields are calculated and phase relations determined, has been successfully used for outlining a conductivity structure consisting of horizontal layering. Although theoretical work has been done on such discontinuities as a vertical fault (d'Erceville and Kunetz[6], Weaver[30]) and a vertical dike (Rankin[15], it has not been successfully applied.

With a single variograph station, the subsurface conductivity is partially indeterminate, but when a series of simultaneous observations is made at a number of stations so that the horizontal distribution of a magnetic variation is known, both a layered structure and horizontal variations may be determined.

The layered structure may be found from a field relation (Price[14]) which gives the ratio of orthogonal horizontal

electric and magnetic field components from the three orthogonal magnetic components. Standard magnetotelluric curves are then used. This procedure has not been found as satisfactory as the normal magnetotelluric technique in which the electric field component is measured by earth electrodes.

In order to investigate the horizontal changes in conductivity it is necessary to determine the induced secondary magnetic field produced by induced currents in the structure. If the horizontal change in conductivity is indicated by anomalous observed field variations of limited spatial extent, the simplest method of separating that part of the field resulting from the conductivity variation from the normal field, (given by the external field plus that due to induction in a uniform layered structure), is to subtract the normal field found at a nearby station from the total measured field. Interpolation between stations on either side of the anomalous region may also be used. This method, of course, assumes relatively uniform external fields over the region considered.

A technique for separating any observed magnetic variation into external and internal parts, using the potential method of Gauss, has been applied by Schmucker[21], and others. A necessary condition in this method is that, at the surface of the Earth, the magnetic variations may be derived from a potential function. This implies that there must be no appreciable current flow between the ionosphere and the Earth.

If one considers the potentials to be expressed as a Fourier series of harmonic components, each decaying exponentially with depth, the potential due to external currents may be expressed in the form

$$V_e(x,z) = -\sum_{n=1}^{\infty} e^{-nz}\left(\frac{A_n}{n}\sin nx - \frac{B_n}{n}\cos nx\right) \quad \text{for } z \geq 0$$

where x is measured in the horizontal direction of the field variation and z vertically downward. The potential due to internal induced currents may be similarly expressed in the form

$$V_i(x,z) = \sum_{n=1}^{\infty} e^{nz}\left(\frac{a_n}{n}\sin nx + \frac{b_n}{n}\cos nx\right) \quad \text{for } z \leq 0$$

The total field components at the surface are then

horizontal $$F(x) = \sum_{1}^{\infty} (b_n + B_n)\sin nx + (-a_n + A_n)\cos nx$$

vertical $$Z(x) = \sum_{1}^{\infty} (-a_n - A_n)\sin nx + (-b_n + B_n)\cos nx$$

From a Fourier analysis of the spatial distribution of the local magnetic variations, the coefficients may be found for

each Fourier component from the relations

$$F(x) = A_n - a_n \qquad Z(x) = B_n - b_n, \quad nx = 0$$

$$F(x) = B_n + b_n \qquad Z(x) = -A_n - a_n, \quad nx = \pi/2$$

Another procedure for separation, which permits total internal and external components of a field variation to be determined requires an estimation of the world wide distribution of magnetic potential during a magnetic disturbance. Chapman and Bartels[3] have determined a world wide average of the ratio of internal to external parts, making a spherical harmonic analysis of the potential distribution and discussing the relation between the various coefficients of the external and internal parts. Rikitake[19] has determined the ratio at each magnetic station by approximating the potential by that obtained from two pairs of radially opposed dipoles, one outside the Earth for the potential associated with external currents and one inside the Earth for the potential associated with the internal induced currents.

Once that part of the observed field variations which is produced by the conductivity inhomogeneity has been determined, it may be compared with the field to be expected from various idealized geometrical structures. The induced field has been given for a sphere (Wait[27], a cylinder (Whitham and Anderson[32] and Wiese[33] and a vertical fault and a vertical dike (d'Erceville and Kunetz[6], Rankin[15], Weaver[30], and Coode[5]).

II. LOCATION AND INSTALLATION OF INSTRUMENTS

Geomagnetic Variographs were set up at 12 stations approximately 80 kilometers apart along an east-west profile from Vancouver, British Columbia to Lethbridge, Alberta (Figure 1). The direction and location of the profile were chosen to be approximately magnetic east-west and to be perpendicular to the Canadian Cordillera. The east-west direction maintains a constant distance from the auroral zone and thus should minimize any differences in external field variations at different stations. The profile was established across the strike of the geological structure in an attempt to be perpendicular to, and to intersect any anomalous conductivity zones. The southern Trans-Canada Highway parallels the profile and provided easy access to the stations.

Variograph locations were chosen with the following requirements:

1. Freedom from local magnetic disturbances. An attempt was made to keep the detector units at least 100 meters from any large quantity of stationary magnetic material and several hundred meters from any moving magnetic material such as automobiles or trains.
2. Reliable 110 volt, 60 cycle line power supply.
3. Easy access by road for the transport of heavy instruments.
4. Satisfactory shelter. This was particularly important for the fluxgate electronic units.
5. Available personnel to make periodic checks and to

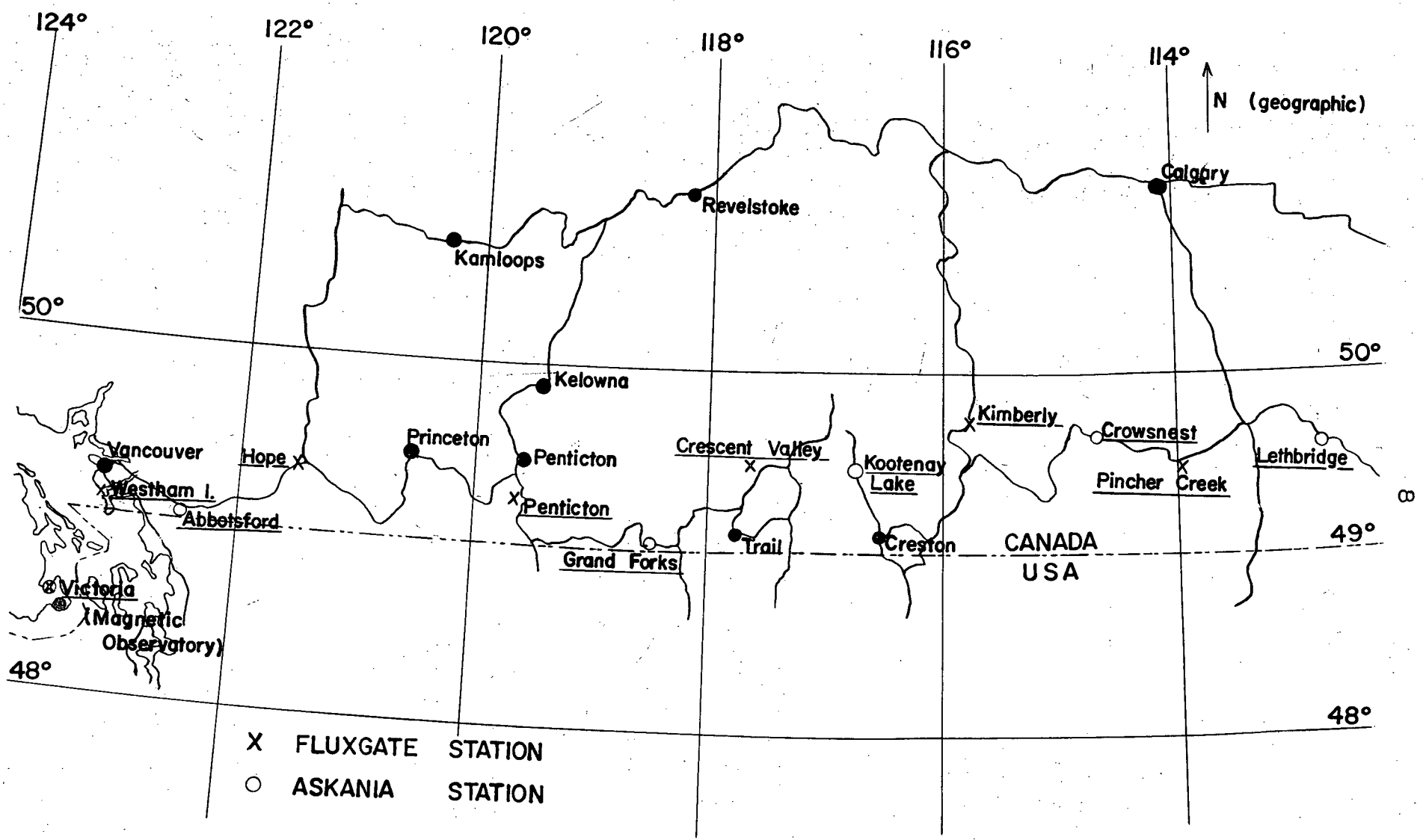

Figure 1. Location Map Showing Sites of Recording Stations

provide maintenance.

At 7 of the 12 sites, cooperation was received from the Department of Transport weather station, aeradio station and airport personnel. Other locations were attended by local residents and employees of business enterprises. The instruments were set up by a two man party which also visited each location at least once a week.

Initially the instruments were set up from Westham Island (Vancouver) to Kootenay Lake. These were operated from June 15 to July 11, 1963. By July 16 the western four stations were moved on to complete the profile to Lethbridge. The intervening stations were operated throughout both phases of the program. Removal of all the instruments was commenced on August 5, 1963. The location of each station and its period of operation are given in Appendix I.

III. DESCRIPTION AND OPERATION OF THE INSTRUMENTS

1. Askania variographs

In 1962 four Askania variographs were purchased by the National Research Council of Canada from the Askania Werke Division of Continental Elektroindustrie of Berlin, Germany for use in upper mantle studies. They were loaned along with four Serson type fluxgate units to the University of British Columbia. The Askania instruments required a minimum of shelter and maintenance and gave excellent records throughout the program. Figure 2 shows the variograph and switchbox units.

Although battery operation is possible with these instruments, line power is needed for any extended operation of the thermostat and heater which are used to maintain a constant instrument temperature. Line power of 60 cycles, 110 to 120 volts was used at all stations. The D (magnetic east-west) and H (magnetic north-south) magnet systems are factory temperature compensated but the Z (vertical) system requires adjustment for different values of the vertical field. The Z magnet system is suspended by two horizontal fibers with different thermal properties. By adjusting their relative stresses, temperature induced deflections may be effectively eliminated. Seven days were spent at the Victoria Magnetic Observatory making this adjustment. The compensation was then found to be sufficient to eliminate any deflection on the

magnetic trace that might be caused by the small temperature variations permitted by the thermostat. Several subsequent power failures indicated that more precise adjustment would be required if the instruments were to be operated effectively without the heater and thermostat.

Since the drive motor supplied with the instruments required 50 cycle power, a gravity drive mechanism was used to transport the recording photographic paper. This provided the additional advantage that during a power failure, although no traces would be produced, the film motion would continue, thus preserving the time scale. The drive could operate unattended for one week at a chart speed of 2 cm/hr.

The three magnetic components H, D and Z , the instrument temperature and a baseline were recorded on 120 millimeter wide photographic paper, "Oscillox" from Technophot Dr. Rudolf Fischer Kg., Berlin - Neukölln. A 10 meter roll filled each magazine, and this was sufficient for 20 days of operation. Two magazines were used with each instrument, so that one could be operated while the other was being processed. Developing was done with Kodak "Dektol" developer, an acetic acid stop bath and Kodak general purpose fixer. The paper was washed with a Kodak hypo clearing agent.

Calibration of the variograph components was provided by built-in Helmholtz coils around each magnet system, a small 1.5 volt battery and an ammeter rheostat system in the switch box.

Hourly time marks were produced on the photographic paper by an auxiliary lamp actuated by German Unghans J chronometers.

1.1 Accuracy and details of variograph records

The light beam for each magnetic component is split into three by reflection and transmission with half silvered mirrors so that the width of the photographic paper may be covered three times. The effective range is therefore approximately 1000 gammas (γ) at a scale value of 3 γ/mm. Some difficulty is encountered in measuring features extending beyond the range of one light spot since the position of one spot when the next appears is not precisely known.

The Helmholtz coil factors are given by the manufacturer to be within $\pm$ 0.7 γ/mm., the ammeter could be read to within $\pm$ 0.005 ma. at 1 or 2 ma., and the deflection distance on the trace could be measured to within about $\pm$ 0.3 mm. at 25 or 50 mm. The overall calibration accuracy is then about $\pm$ 0.04 γ/mm. for all components. Differences as large as 0.04 γ/mm. were observed between calibrations at the top and bottom of the range of a single light trace while for different light traces of the same component the difference in calibration values was as large as 0.15 γ/mm.

The time marks were found to have less than 0.5 minutes parallax with the component traces. The chronometers were maintained by W.W.V. or C.H.U. short wave time signals to less than 1.5 min. error. Records were also kept of the gain or

loss by each chronometer so that times may be determined on the traces to within ± 0.8 min.

1.2 Poor or lost records

On several occasions wind noise was superimposed on the traces of instruments which were covered only by plywood shelters (Figure 2). This was particularly evident at Lethbridge where an exposed location was subject to winds up to 75 km/hr.

Time marks were lost for a week at one station because of a break in the chronometer connecting cable and for a week at another because the chronometer stopped.

Record was lost for a number of periods at the Kootenay Lake Station because of an unreliable line power supply. A period of several hours was required after power restoration before a constant temperature could be maintained by the heater.

At several stations the air temperature occasionally rose above the thermostat setting and fluctuations in instrument temperature resulted. The thermostatically controlled temperature was also found to change occasionally because of unexplained effects within the thermostat system.

Each variograph was set up either on an existing concrete floor or on concrete pads laid before the installation so that drifts in level and in orientation were present only during the first few days of operation.

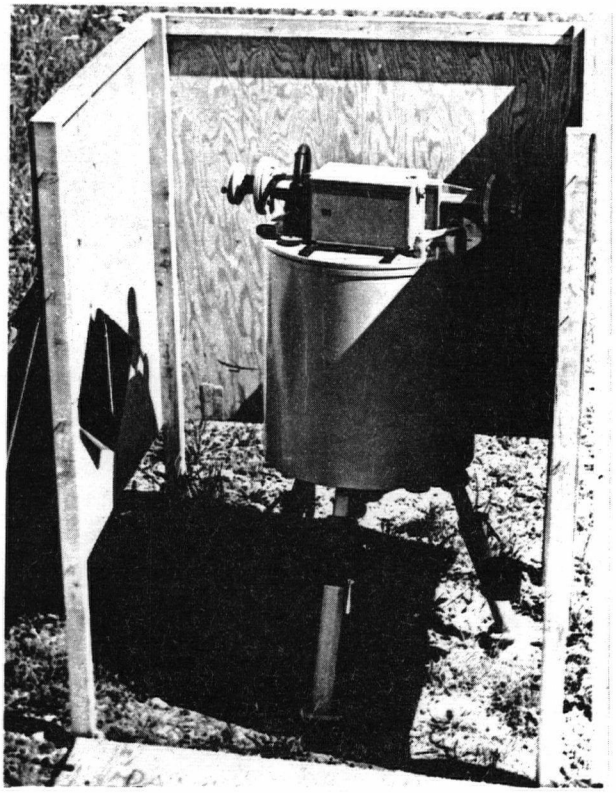

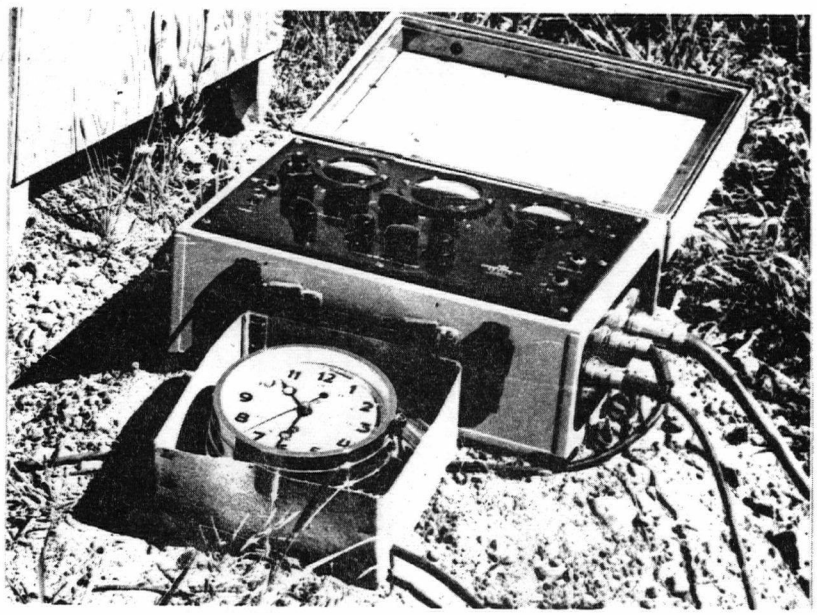

Figure 2. Askania Variograph and Switchbox.

2. Fluxgate recording magnetometers

The four fluxgate type recording magnetometers were of the type designed by Serson[23] for the Dominion Observatory and built by Canadian Applied Research Limited during the International Geophysical Year (Figure 3). The instruments consist of a three component detector head which may be set up outside away from local magnetic disturbances and an electronic assembly and recorder which are connected to it by a 6 conductor cable. The output of the magnetometer is 3 d.c. voltages which are proportional to the three magnetic field components at 10 v./1000 γ . The constant portion of the field is balanced by adjustable and calibrated bias voltages. A Sorensen a.c. voltage regulator was used to prevent any drift of the traces caused by poor stability in the line power supply.

Leeds and Northrup 6 channel Speedomax type G, model S, 6000 series recorders with a full scale deflection of 10 mv. were used. Channels 1 and 4, 2 and 5 and 3 and 6 were connected in parallel except at one station (Penticton) where earth currents were also measured, so that a point was printed every 9 seconds on the trace for each component. The chart speed was set at 1 in./hr.

2.1 Accuracy and details of fluxgate records

An attenuation potentiometer circuit was used to reduce the input to the recorder by a factor of 500 giving a sensitivity of 50 γ/in. or 500 γ full scale. With the accuracy of the

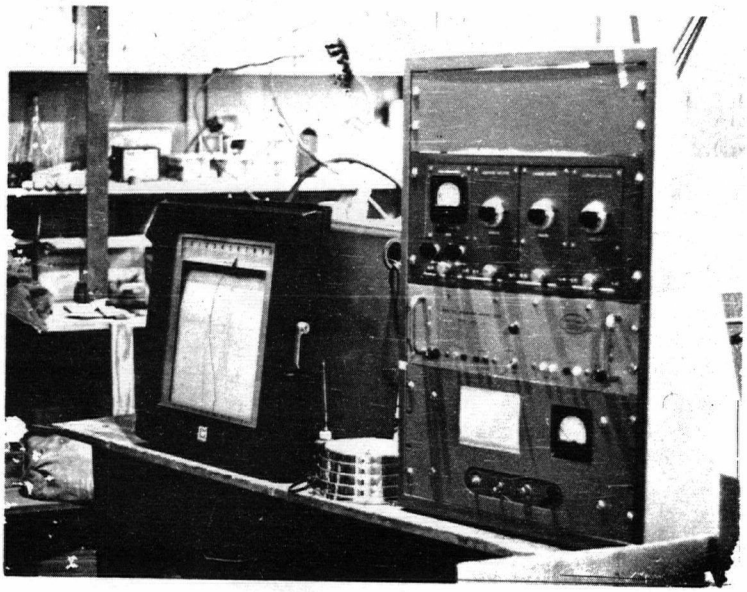

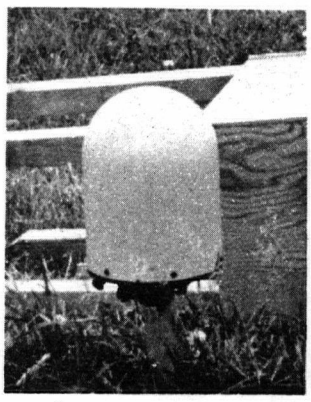

Figure 3, Fluxgate Recorder, Electronics and Detector Head.

output of the magnetometer given by Serson as within ± 1% and 1% resistors in the potentiometer, this calibration should be accurate to within ± 4%. Approximate timing was provided by the one inch grid on the chart and more precisely by Unghans J chronometers actuating a marking pen on the side of the chart paper. Times on the traces could be determined to within ± 3 minutes.

2.2 Poor or lost records

The major problem encountered with the fluxgate units was long period drift. This was particularly evident at the Penticton station where the D component exhibited daily variations exceeding 500 γ. Several other units showed daily drifts of up to 100 γ, particularly in the $\bar{z}$ component. The diurnal magnetic variation for the period of the study should be about 30 γ. These drifts appear to be the result of a temperature induced effect in the detector elements. A thermostatically controlled case or shelter is suggested for any future use of these instruments.

The detector heads were mounted on 1-3/8 in. aluminum tubing set in concrete. This permitted negligible drifts in level or orientation but disalignments did result from jarring by people and animals.

Record was also lost because of trouble with the recorder. On two units a small stop behind the potentiometer split drive gear loosened and jammed the pen carriage. On another there was slipping of the actuating wheels for the printing pen.

It should be noted that in a comparison between the Askania and fluxgate units, the Askanias gave good results for magnetic variations with periods from 5 min. to 24 hr. with narrow uniform traces, and almost no record lost, while the fluxgates with Leeds and Northrup recorders gave fair results for periods from 15 min. to 2 hr., with wide irregular traces and an average of 5 days of record lost on each instrument operating over a period of 6 weeks.

3. Proton precession magnetometer

A small battery operated proton precession magnetometer was received on loan from the Dominion Observatory magnetic station, Victoria, B.C. This was a model G.M.-102 made by Barringer Research of Toronto Ontario, with a direct reading of total field to 10 γ . Readings were generally reproducible to within $\pm$ 20 or 30 γ . At each Askania or fluxgate station, nine readings were taken on a square 100 ft. grid with the set up at the center, to ensure that there were no large magnetic bodies near the site and to determine the total field intensity at the station.

4. Earth currents

An attempt was made to record the time variation in the potential difference between two 500 ft spaced buried copper electrodes at the Penticton and Crescent Valley stations. Together with the magnetic records these could be used in

magnetotelluric studies. The Crescent Valley measurements were unsuccessful because of local potentials induced in the ground by a nearby buried teletype cable. The potential induced by this cable was much greater than that induced by external magnetic variations for a distance of at least 500 ft. from the cable. At Penticton the potential difference was recorded for magnetic east-west and magnetic north-south electrode pairs for a three week period. Two channels on the Leeds and Northrup recorders were used. Very scattered traces were obtained, and no analysis has been undertaken of these results.

IV. INDUCTION ANALYSIS

1. Induced currents in a uniform Earth

The magnetic variations which are observed at the surface of the Earth have been found to arise partly from currents in the ionosphere and partly from currents induced in the Earth by these external sources. For an Earth of infinite conductivity, the induced or inner field opposes and completely cancels the vertical component of the external field at the Earth's surface but aids and doubles the horizontal component. A simple application of images gives the required result. Considering an external line current source, the boundary conditions are satisfied by an image source within the Earth with opposite direction of current flow.

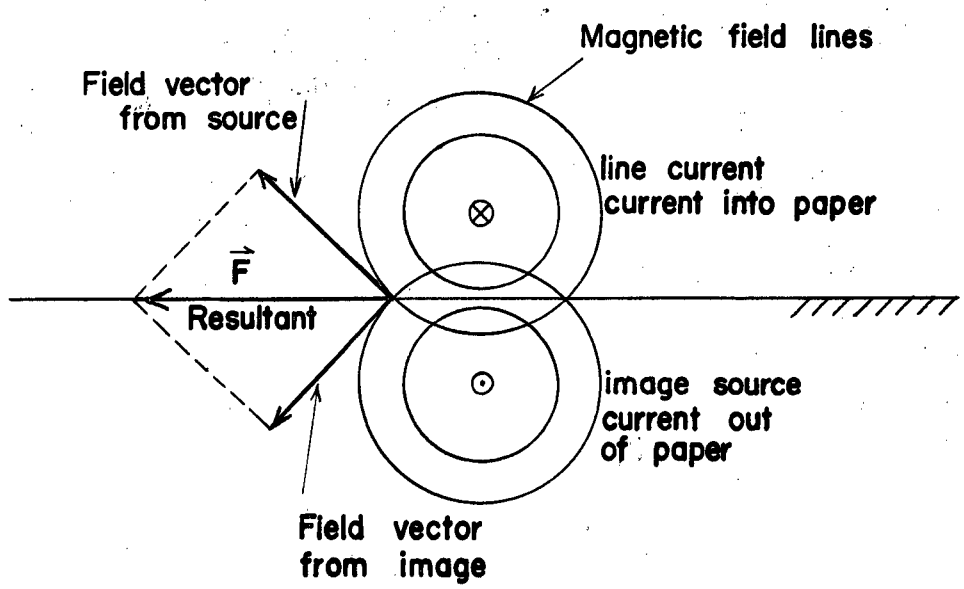

Figure 4. Image Source Representation of Induction in a Uniform Earth of Infinite Conductivity.

If the conductivity is finite, the same image representation holds except that the image current is not as strong as the external source. The horizontal component is still increased and the vertical decreased, although the vertical component is not completely cancelled.

Snell's Law may be applied to the Earth-air boundary to determine quantitatively the extent to which the incident external field is increased in the horizontal and decreased in the vertical direction.

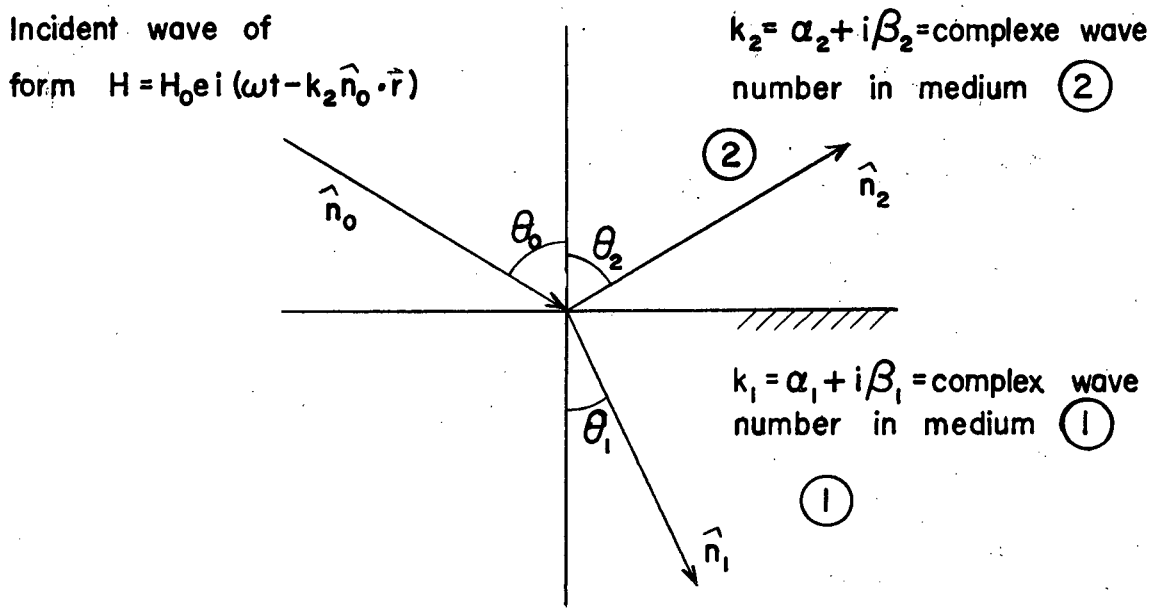

Figure 5. Application of Snell's Law to the Earth-Air Boundary.

By Snell's Law

$$k_1 \sin\theta_1 = k_2 \sin\theta_2$$

For a nonconductor such as air

$$\alpha_2 = \omega\sqrt{\mu_0 \epsilon_0}\,, \qquad \beta_2 = 0 \qquad \text{(M.K.S. Units)}$$

and for a conductor such as the Earth

$$\alpha_1 = \beta_1 = \sqrt{\frac{\omega\mu_1\sigma_1}{2}}$$

The angle of the refracted wave is then given by

$$\sin\theta_1 = \sin\theta_0 \left[\sqrt{\frac{2\omega\mu_0\epsilon_0}{\mu_1\sigma_1}} \quad \frac{1}{1+i} \right]$$

As the conductivity of the Earth, σ_1, increases, $\sin\theta_1 \longrightarrow 0$ and the field measured at the surface of the Earth is equivalent to a vertically incident field.

The amplitudes of the reflected and transmitted fields at the surface may then be determined by applying Fresnel's equations. In terms of the incident wave they are found to be

Reflected $$R = \frac{1}{\mu\omega} \frac{k_2^2 \cos\theta_0 - k_1 k_2 \cos\theta_1}{k_2 \cos\theta_0 + k_1 \cos\theta_1}$$

(if $\mu_1 = \mu_2$)

Transmitted $$T = \frac{1}{\mu\omega} \frac{2 k_2 \cos\theta_0}{k_2 \cos\theta_0 + k_1 \cos\theta_1}$$

The magnetic disturbance vector is assumed to be in the plane of the above diagram.

2. Induction in conductivity inhomogeneities

The analysis of the conductivity and geometry of zones causing anomalous magnetic field variations involves correlating the induced secondary field produced by the conductivity inhomogeneity with the incident field. The intensity and nature of the incident field will depend on the external ionospheric

current sources and on the currents produced by these external fields in the Earth external to the zone. Provided some estimate can be made of the depth to the inhomogeneous zone and of the changes in conductivity with depth in the surrounding region, good estimates may be made of the field incident on the inhomogeneity. A more common assumption is that the incident field is the same as that measured at the surface away from the influence of the inhomogeneity. This requires that the depth to the anomalous zone is much less than the skin depth of the surrounding Earth for the periods of the magnetic variations used.

Under this assumption, and provided that the induced field components are independent of each other, 18 correlation coefficients are required to completely specify the correlation between the inducing and induced fields. This includes the possibility of in phase and out of phase components in the induced field. A knowledge of these coefficients for all periods of field variation completely specifies the information available from a single variograph station. To outline such three dimensional bodies as a sphere is thus quite difficult unless simplifying assumptions are made.

If the region of inhomogeneous conductivity is two dimensional, only those components of field variations perpendicular to the strike of the region should be effective in producing induced currents. Once this strike is known, 8 correlation coefficients are left to be determined. Assuming

a linear relation between the induced currents and the normal field components (ohmic resistance) and a horizontal two dimensional zone, the defining relations for a harmonically varying field

$$F_n = F_{n_1} \sin \omega t + F_{n_2} \cos \omega t$$ normal horizontal (perpendicular to the strike of the zone)

$$F_a = F_{a_1} \sin \omega t + F_{a_2} \cos \omega t$$ anomalous horizontal (perpendicular to the strike of the zone)

$$Z_n = Z_{n_1} \sin \omega t + Z_{n_2} \cos \omega t$$ normal vertical

$$Z_a = Z_{a_1} \sin \omega t + Z_{a_2} \cos \omega t$$ anomalous vertical

are

$$Z_{a_1} = A_1 F_{n_1} + B_1 Z_{n_1} + A_2 F_{n_2} + B_2 Z_{n_2}$$

$$Z_{a_2} = A_2 F_{n_1} + B_2 Z_{n_1} + A_1 F_{n_2} + B_1 Z_{n_2}$$

$$F_{a_1} = C_1 F_{n_1} + D_1 Z_{n_1} + C_2 F_{n_2} + D_2 Z_{n_2}$$

$$F_{a_2} = C_2 F_{n_1} + D_2 Z_{n_1} + C_1 F_{n_2} + D_1 Z_{n_2}$$

where A_1, B_1, C_1, D_1 refer to the components of the induced field in phase with the inducing field and A_2, B_2, C_2, D_2 refer to the out of phase components.

To utilize geomagnetic variation data, the time varying fields must be transformed into harmonic terms, either by estimating the dominant harmonic component of each of a number of magnetic variation features or by expressing the magnetic changes as frequency functions by Fourier transforms.

i.e. $$Z(t) = \frac{1}{\sqrt{2\pi}} \left[\int_{-\infty}^{\infty} A(\omega) \cos\omega t \, d\omega + \int_{-\infty}^{\infty} B(\omega) \sin\omega t \, d\omega \right]$$

The frequency functions $A(\omega)$ and $B(\omega)$ represent spectral densities of harmonic functions and may be used in the same manner as true harmonic time functions.

Once the correlation coefficients have been determined as a function of period, a comparison may be made with those to be expected for any idealized geometry and conductivity configuration.

3. Condition for in phase induction

The above computations are greatly simplified if the induced field is in phase with the incident inducing field, i.e. A_2, B_2, C_2 and D_2 are all small. The condition for in phase induced fields may be expressed in terms of simple circuit elements.

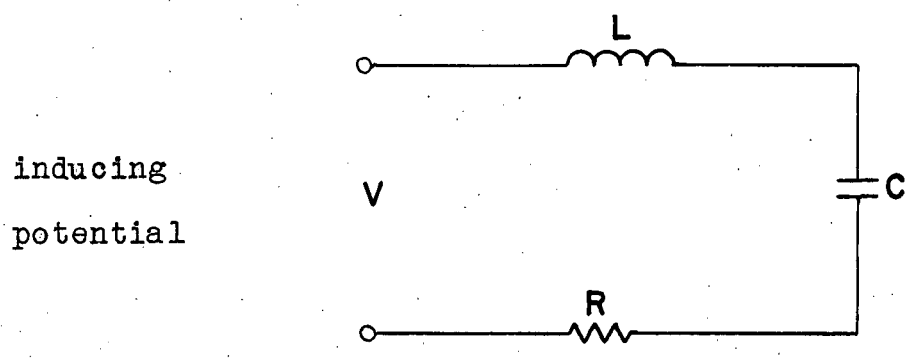

Figure 6. Induction in Terms of Simple Circuit Elements.

For a harmonically varying source $V = V_0 \cos\omega t$, the current induced in the circuit is given by

$$I = V_0 \frac{\left[R\cos\omega t + \left(\omega L - \frac{1}{\omega C}\right) \sin\omega t \right]}{R^2 + \left(\omega L - \frac{1}{\omega C}\right)^2}$$

The inducing potential is proportional to the time rate of change of the external magnetic field B, so that if

$$B_e = B_{e_0} \sin\omega t, \qquad V = (\text{constant})\, B_{e_0} \cos\omega t$$

the induced field is then

$$B_i = (\text{constant})\, B_{e_0} \frac{R\cos\omega t + \left(\omega L - \frac{1}{\omega C}\right) \sin\omega t}{R^2 + \left(\omega L - \frac{1}{\omega C}\right)^2}$$

since the induced field is in phase with the induced current. The conditions for in phase induced secondary fields are then

(i) $\left|\omega L - \frac{1}{\omega C}\right| >> R$

(ii) $\omega L > \frac{1}{\omega C}$ or $\omega^2 LC > 1$

4. Conditions under which the electric field of a source may be neglected.

Any source of a magnetic field variation must produce an associated time varying electric field. Since most sources of magnetic variations may be represented as magnetic dipoles or are closed current systems which may be represented by the superposition of a number of magnetic dipoles, the electric field near the source falls off with the distance squared while the magnetic field falls off with the distance cubed. Thus within one wavelength of the source (near field region) the magnetic field is found to be dominant. For field variations with periods of a few minutes the wavelength is of the order of 10^{11} meters so that all observation points should satisfy this condition.

5. Model calculations.

Since it is difficult to calculate the structure and conductivity contrast resulting in anomalous magnetic variations directly from the induction coefficients, it is

expedient to determine these parameters for various theoretical models and then make comparisons with the observed results. This method provides no guarantee of the uniqueness of the solution but certain configurations are more physically plausible than others.

(i) Cylinder

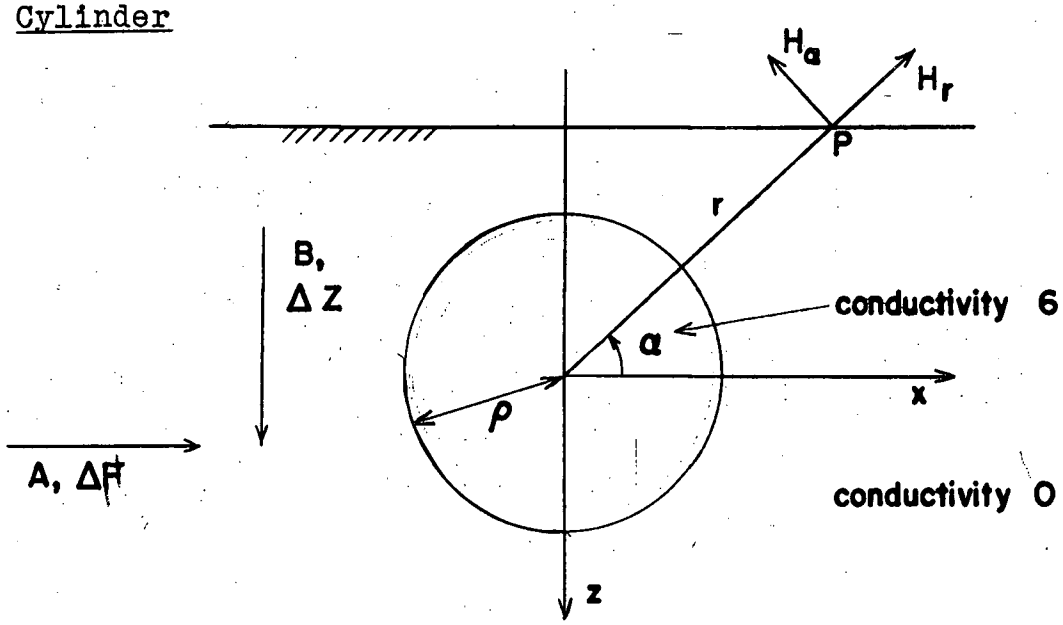

Figure 7. Representation of a Cylinder in a Slowly Varying Magnetic Field.

A magnetic vector potential $\vec{\phi}$ may be chosen such that the magnetic field inside and outside the cylinder is given by

$$\vec{T} = \text{curl}\ \vec{\phi}$$

It is found that $\vec{\phi}$ must satisfy

(a) $\nabla^2 \phi = i\omega 4\pi\sigma\phi$ inside the cylinder

(b) $\nabla^2 \phi = 0$ outside the cylinder

A satisfactory solution in cylindrical coordinates outside the cylinder is given by

$$\phi = \left(r - \frac{I}{r}\right)\left(A \sin\alpha + B\cos\alpha\right)$$

where A and B are the horizontal and vertical components of the potential resulting from the external field, and I is the coefficient of induction in the cylinder. I is dependent on the diameter and conductivity of the cylinder and on the period of the magnetic variations. The radial and azimuthal fields are given by

$$H_r = \frac{1}{r}\frac{\partial\phi}{\partial\alpha} = \left(1 - \frac{I}{r^2}\right)\left(A\cos\alpha - B\sin\alpha\right)$$

$$H_\alpha = -\frac{\partial\phi}{\partial r} = -\left(1 + \frac{I}{r^2}\right)\left(A\sin\alpha + B\cos\alpha\right)$$

The components in the horizontal and vertical directions are thus

$$F = A - \frac{IA}{r^2}\cos 2\alpha + \frac{IB}{r^2}\sin 2\alpha$$

$$Z = B + \frac{IA}{r^2}\sin 2\alpha + \frac{IB}{r^2}\cos 2\alpha$$

These expressions may be solved for α the dip angle to the center of the cylinder using the observed values of

$$F = F_n + F_a, \quad Z = Z_n + Z_a, \quad A = F_n, \quad B = Z_n$$

The induction coefficient I may be found by applying the boundary conditions at the surface of the cylinder to the above solution and to the solution of (a). Only the first mode of oscillation (dipole) need be considered since the wavelength associated with the field variation may be taken to be much greater than the dimensions of the region of measurement. The solution is found to be [9]

$$I = \rho^2 \frac{J_2(\sqrt{-i}\, k\rho)}{J_0(\sqrt{-i}\, k\rho)}$$

where $k^2 = 4\pi\sigma i\omega$ and J_0 and J_2 are Bessel functions of order zero and two respectively. This solution may be separated into in phase and out of phase parts.

$$I = \rho^2 (M + iN)$$

The dependence of these terms on the conductivity and radius of the cylinder and on the frequency of the magnetic variations is given in Figure 10.

If the cylinder is approximated by a perfect conductor $k \to \infty$ and $I \to \rho^2$. The conditions under which this is a satisfactory assumption are given by examination of Figure 10. The induced field components then become

$$Ha = \frac{\rho^2}{f^2} \left[-A \cos 2\alpha + B \sin 2\alpha \right]$$

$$Za = \frac{\rho^2}{f^2} \left[A \sin 2\alpha + B \cos 2\alpha \right]$$

Either of these equations may be used to find the ratio $\frac{\rho}{f}$. The form of the spatial variation of the anomalous induced fields over a highly conducting buried cylinder, assuming a horizontally incident magnetic field variation is given in Figure 8.

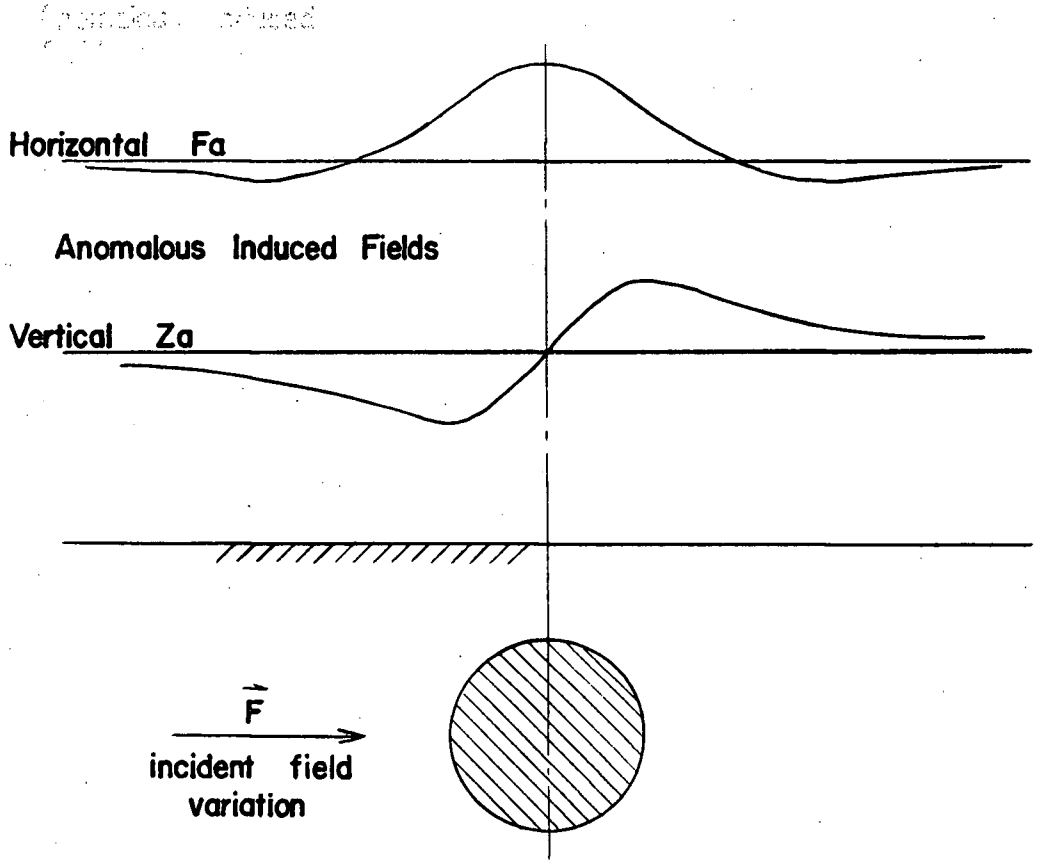

Figure 8. Form of the Anomalous Induced Fields Over a Cylinder for a Horizontal Incident Magnetic Field Variation.

(ii) Sphere

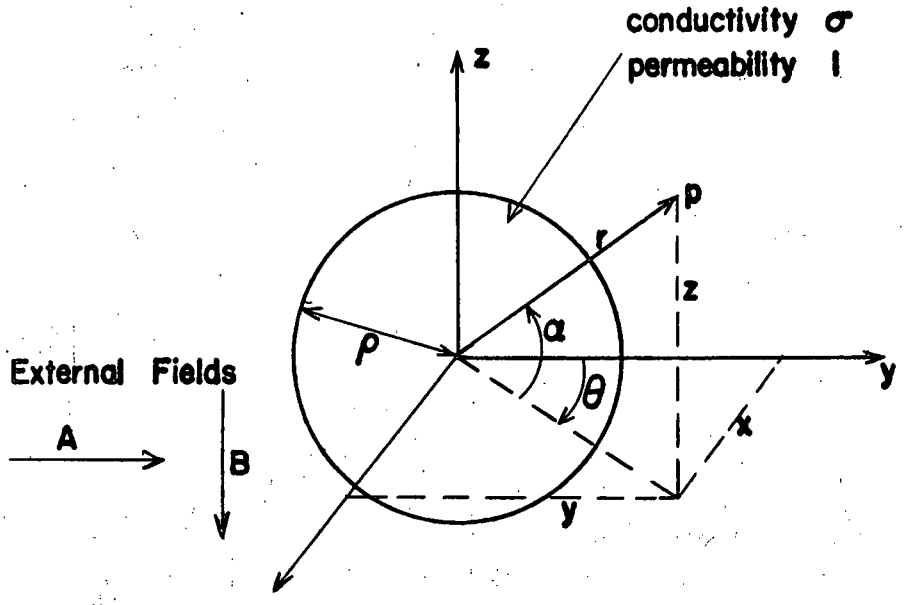

Figure 9. Representation of a Sphere in a Slowly Varying Magnetic Field.

The solution of Laplace's equation for the vector potential, $\nabla^2 \phi = 0$ outside the sphere gives secondary magnetic field components resolved along the axes

$$H_{ya} = \frac{I}{r^3}\left[\left(1 - 3\cos^2\theta\cos^2\alpha\right)A + \left(3\cos\theta\cos\alpha\sin\alpha\right)B\right]$$

$$H_{xa} = \frac{I}{r^3}\left[\left(3\sin\theta\cos\theta\cos^2\alpha\right)A + \left(3\sin\theta\cos\alpha\sin\alpha\right)B\right]$$

$$Z_a\,(down) = \frac{I}{r^3}\left[\left(3\cos\theta\cos\alpha\sin\alpha\right)A + \left(1 - 3\sin^2\alpha\right)B\right]$$

These equations may be solved for α and θ.

Applying the boundary conditions at the surface of the sphere to the above equations and those applicable to the inside of the sphere gives

$$I = \frac{3}{2}\rho^3\left[\frac{1}{\gamma^2} + \frac{1}{3} - \frac{\cosh\gamma}{\gamma\sinh\gamma}\right] \quad \text{where} \quad \gamma^2 = \sigma i\omega$$

This may be separated into in phase and out of phase components

$$I = \frac{3}{2}\rho^3\left[M + iN\right]$$

If the sphere is assumed to have infinite conductivity this becomes

$$I = \frac{\rho^3}{2}$$

and may be inserted into the expressions for the induced field components to give a value of $\frac{\rho}{4}$.

(iii) Horizontally discontinuous structure

No exact solution for the secondary fields produced by a magnetic field variation incident on a horizontally discontinuous structure has been obtained but the following discussion outlines the nature of the anomalous field variations and their orders of magnitude[29].

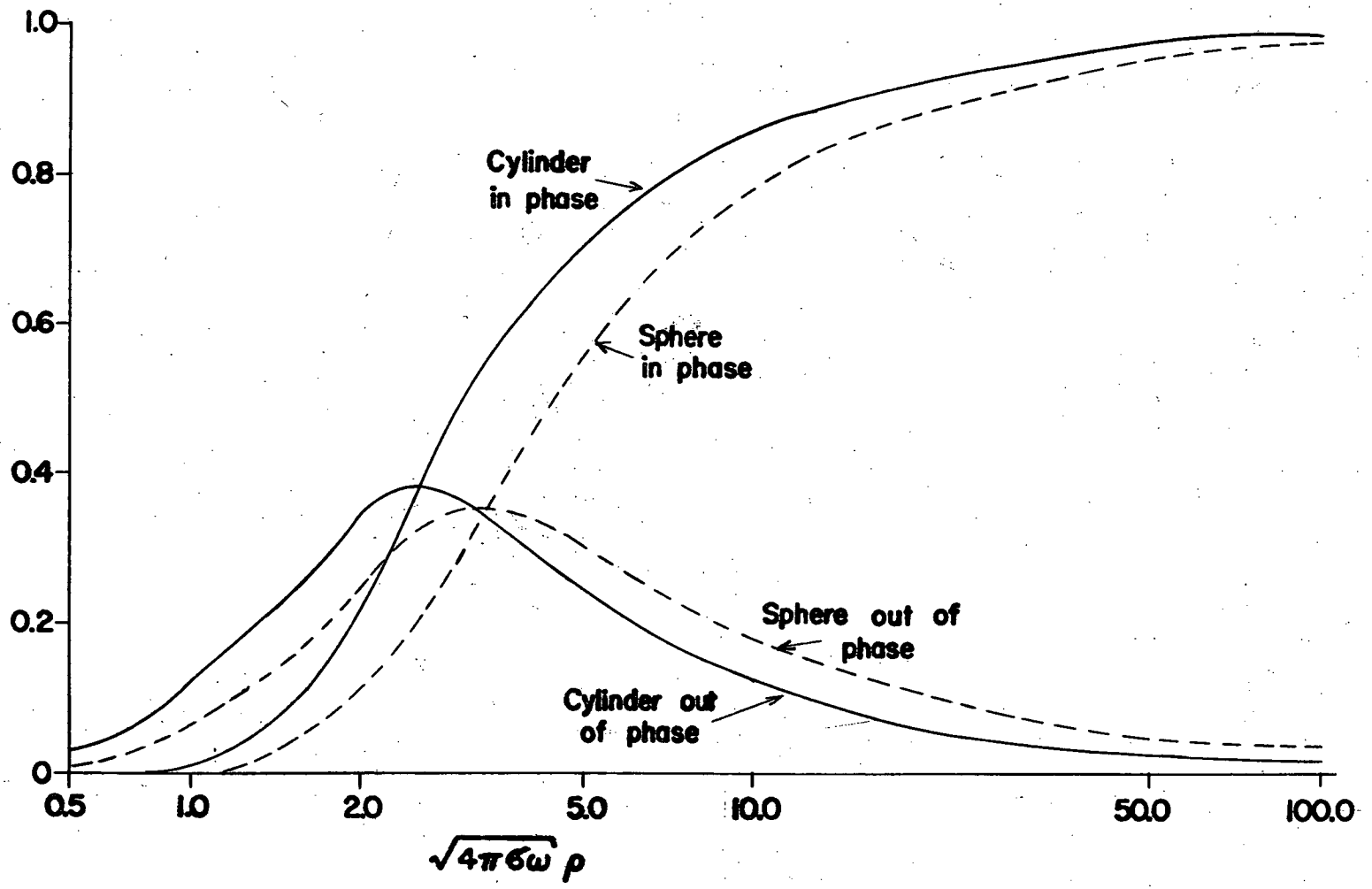

Figure 10 In Phase and Out of Phase Induction Coefficients for a Conducting Cylinder and Sphere

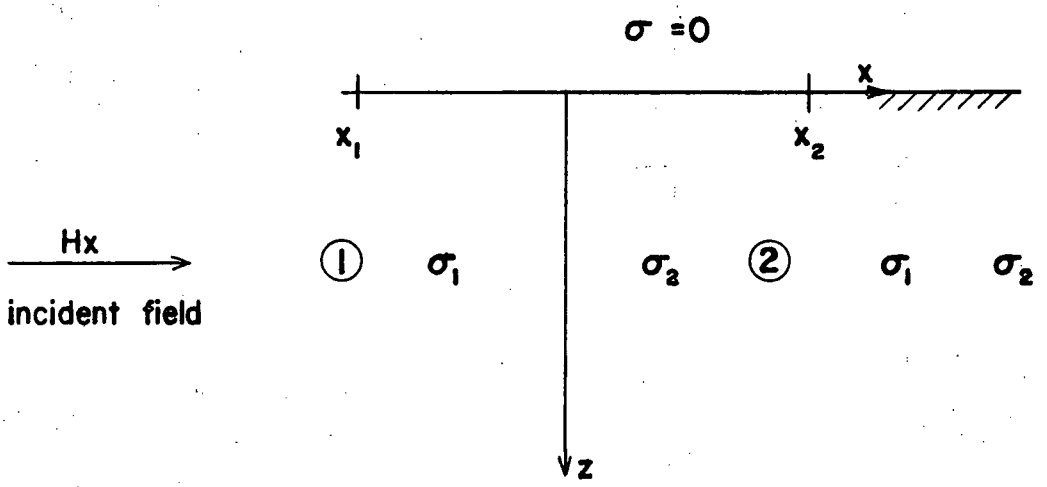

Figure 11. Representation of a Horizontally Discontinuous Structure.

At places sufficiently far from the interface $x = o$, i.e. $x < x_1$, or $x > x_2$, the electric and magnetic fields should be approximately equal to that for a uniform conductor (provided σ_1 and σ_2 are both sufficiently large that most of the incident fields are reflected in both cases). The attenuation of the magnetic field with increasing depth in a conductor such as the Earth may be determined from the diffusion equation

a) $$\frac{\partial^2 H_x}{\partial z^2} = \frac{4\pi i \omega \sigma H_x}{c^2}$$ (in gaussian units)

thus b) $H_x = 2H_0\, e^{-pz}$ where $p^2 = \frac{1}{c^2}\, 4\pi\sigma i\omega$ and $2H_0$ is the field at the surface $z = 0$.

Since $\sigma_2 > \sigma_1$ the field is stronger in ① than ② because there is less reflection of the incident field in ① than in ②. The electric field in the Earth will be governed by the diffusion equation

c) $\nabla^2 E_y = \frac{4\pi\sigma}{c^2}\, \frac{\partial E_y}{\partial t}$ where $\frac{c^2}{4\pi\sigma} = D$, i.e. the diffusion constant.

The E_y field thus diffuses from ① to ②. From Maxwell's second equation

d) $\frac{\partial E_y}{\partial x} = \frac{1}{c}\, \frac{\partial H_z}{\partial t}$

it follows that a vertical magnetic field should be associated with this diffusion.

An order of magnitude estimate of H_z at the surface $z = 0$ may be obtained by replacing $\frac{\partial E_y}{\partial x}$ by $\frac{\Delta E_y}{x_2 - x_1}$ in (d).

Take

$$\Delta E_y = E_y(x_2) - E_y(x_1)$$

but from $\vec{\nabla} \times \vec{H} = 4\pi \frac{\sigma}{c} \vec{E}$, Maxwell's first equation,

$$E_y = \frac{c}{4\pi\sigma}\, \frac{\partial H_x}{\partial z}$$

and from (b) $\frac{\partial H_x}{\partial z} = -2H_0\, p\, e^{-pz}$

At the surface then

$$\Delta E_y = H_o \frac{\sqrt{\omega}}{\sqrt{\pi}} \left[\frac{1}{\sqrt{\sigma_1}} - \frac{1}{\sqrt{\sigma_2}} \right]$$

The width of the transition zone $x_2 - x_1 = L$ may be approximated by $\sqrt{DT}$ (where T is the period of the field variation), which is the characteristic distance over which the difference in field intensity should be eliminated in one period. The diffusion constant may be taken as $D = D_1$, since the rate of diffusion is faster in ① than ② . Thus

$$L \approx c\sqrt{\frac{T}{4\pi\sigma_1}} = \frac{c}{2\pi\sqrt{2\omega\sigma_1}}$$

The anomalous H_z at the surface may then be found from (d) to be

$$|H_z| = \sqrt{2\pi} \left[1 - \frac{\sigma_1}{\sigma_2} \right] 2H_o$$

where $2H_o$ is the approximate horizontal field intensity distant from the discontinuity.

The horizontal field measured at the surface away from the discontinuity is

$$H_x = 2H_o \left(1 - \frac{k\sqrt{i}}{\gamma} \right) \qquad k = \frac{\omega}{c} \qquad \gamma = \sqrt{4\pi\sigma\omega}$$

thus if $k \ll \gamma$, which requires that ω be small and δ large, H_x is independent of δ and there is no horizontal variation across the discontinuity. If this condition is not satisfied, the magnitude of the anomalous H_x has not been satisfactorily determined.

V. RESULTS AND ANALYSIS

1. General results

(i) Pulsations (0.5 to 5 min. period)

Geomagnetic variations with periods from 0.5 to 5 min. could be observed only on the Askania records. No conductivity inhomogeneity indicated by anomalously large vertical components was observed at the four western Askania stations, Abbotsford to Kootenay Lake. The ratio of the amplitude of features in the horizontal direction to those in the vertical direction is 5 to 1 or greater. The Victoria Magnetic Observatory and the two eastern stations, Crowsnest and Lethbridge, show much larger vertical amplitudes. The horizontal to vertical amplitude ratio is around 2 to 1. There is also some correlation between the horizontal and vertical magnetic traces. This suggests a conductivity anisotropy in the near surface layers. Such an anisotropy has been demonstrated by Srivastava et al[24] in southwestern Alberta through magneto-telluric and telluric measurements. The results at Victoria could be caused by the nearby land-sea contact. Christoffel et al[4] have found similar results in micropulsation studies extending from Victoria, inland. Because of the very small amplitudes of the features of these periods on the magnetograms, no detailed analysis has been attempted.

(ii) Bays and Storm Features (5 to 120 min.)

For geomagnetic disturbances with periods between 5 and 120 min., the records from the western 7 stations Victoria to Grand Forks, were normal. The ratio of horizontal to vertical amplitudes is generally around 5 to 1. For the eastern 6 stations, Crescent Valley to Lethbridge, the vertical amplitudes are much larger, with the ratio being about 2 to 1. In general the horizontal components are similar across the profile, with the vertical components at these last 6 stations differing widely.

At these eastern 6 stations a correlation is also apparent between the horizontal and vertical magnetic traces. This suggests that the large vertical amplitudes are caused by currents induced, largely by the horizontal disturbance, in conductivity inhomogeneities . With increasing period the induced vertical component shows decreasing amplitude. At 60 min. it is about half that at 10 min.

In addition to these effects that part of the vertical component which is present at all stations appears to increase with increasing period. This suggests that either the ionospheric current systems responsible for the longer period features produce a greater vertical magnetic component than those responsible for the shorter period ones or that the conductivity is lower at the greater depths penetrated by the long period variations. The latter possibility does not agree with the results of Srivastava[24], Niblett[12] and Cantwell[2]

who found by magnetotelluric methods an increasing conductivity below a depth of about 80 km.

(iii) Diurnal Geomagnetic Variations

The diurnal variations in the geomagnetic field (periods from 6 to 24 hrs.) were examined only at Askania stations since the daily temperature drift of the Fluxgate magnetometers was very pronounced. Two consecutive applications of running means of adjacent values were used to determine the diurnal variations during a quiet day in each period of operation (Figures 12, 13 and 14).

The plots are all similar in the H and D components, but the Z components at different stations show some pronounced differences. At Crowsnest in the central Rocky Mountains, there is a strong morning rise (peak at 0800 L.M.T.) of 25 γ which is not present at the other stations. Since the adjacent Askania stations 150 km. to the east and west show no such behaviour, and since the D and H plots show no differences, it may be reasonably assumed that the external current source is uniform across the profile and that the anomaly is caused by induction effects in the Earth. A mean of four quiet days has also shown that this result is not particular to one day. The anomalous variation is of great interest since a similar effect has been noted by Schmucker[22] in southwestern New Mexico, U.S.A. This is about 2000 km. south of Crowsnest and similarly situated about 600 km. from the coast.

An anomaly not present at adjacent stations and appearing

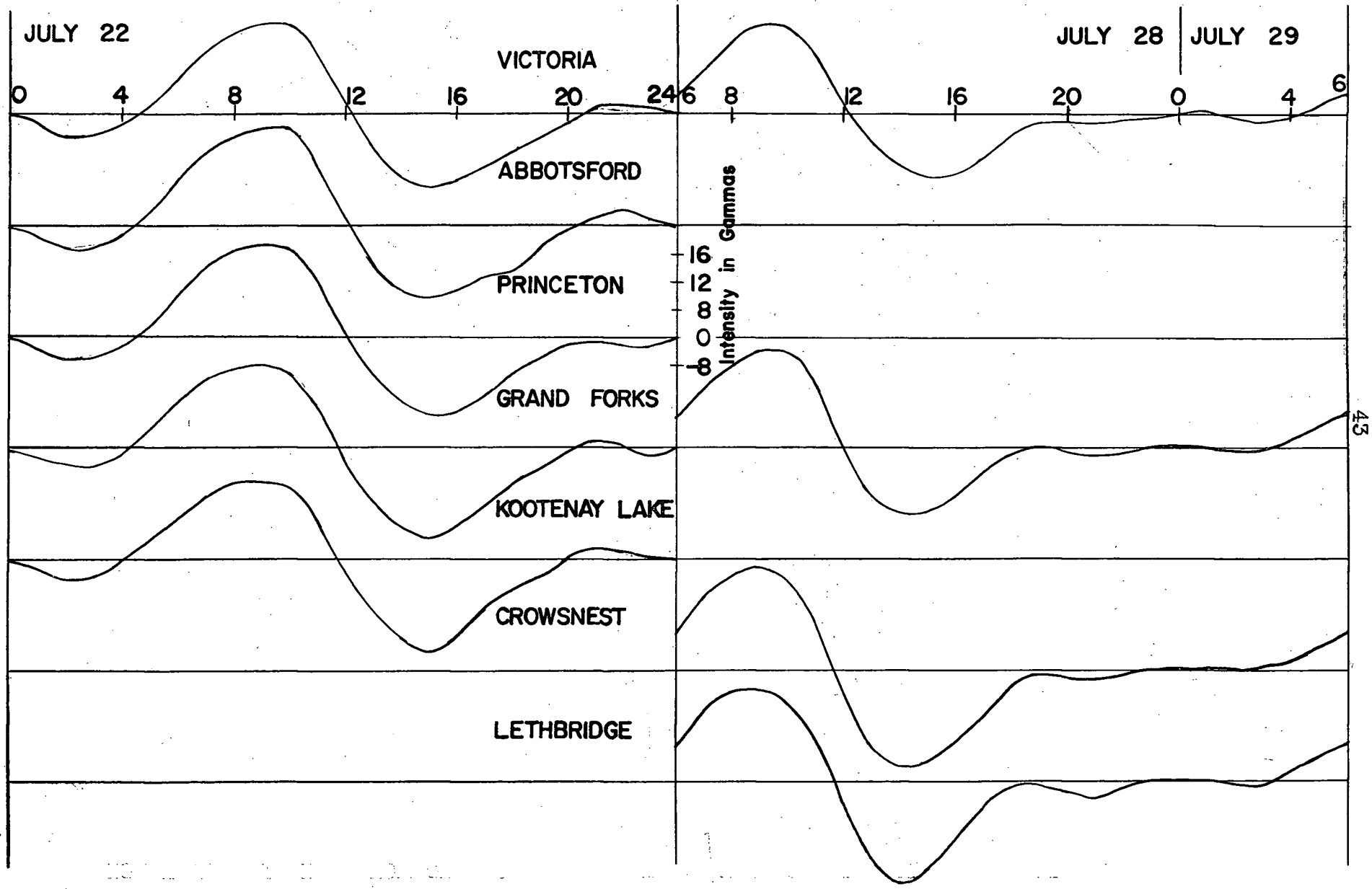

Figure 12. Diurnal Geomagnetic Variations, Magnetic East-West (D) Component

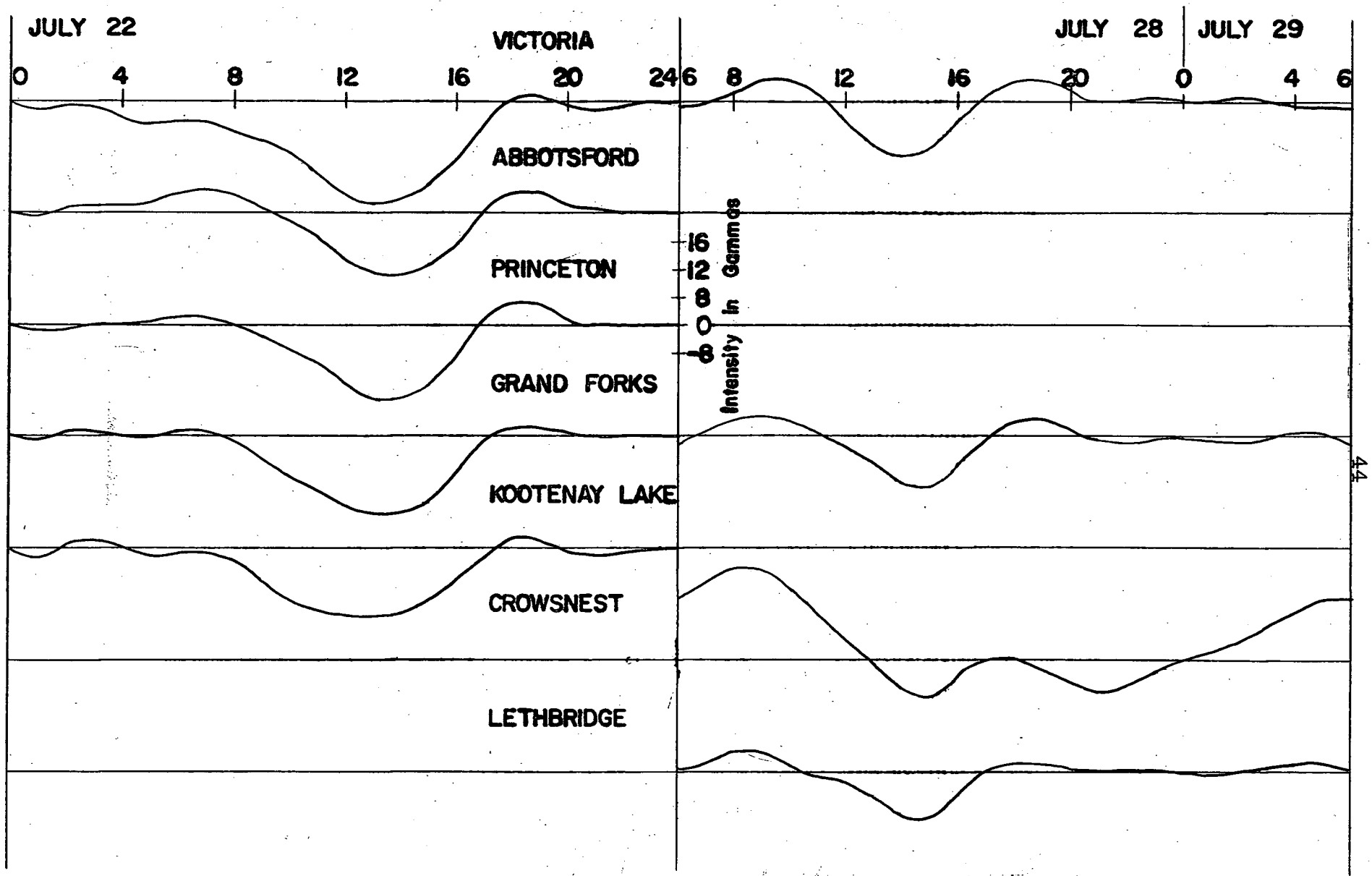

Figure 13. Diurnal Geomagnetic Variations, Vertical (Z) Component

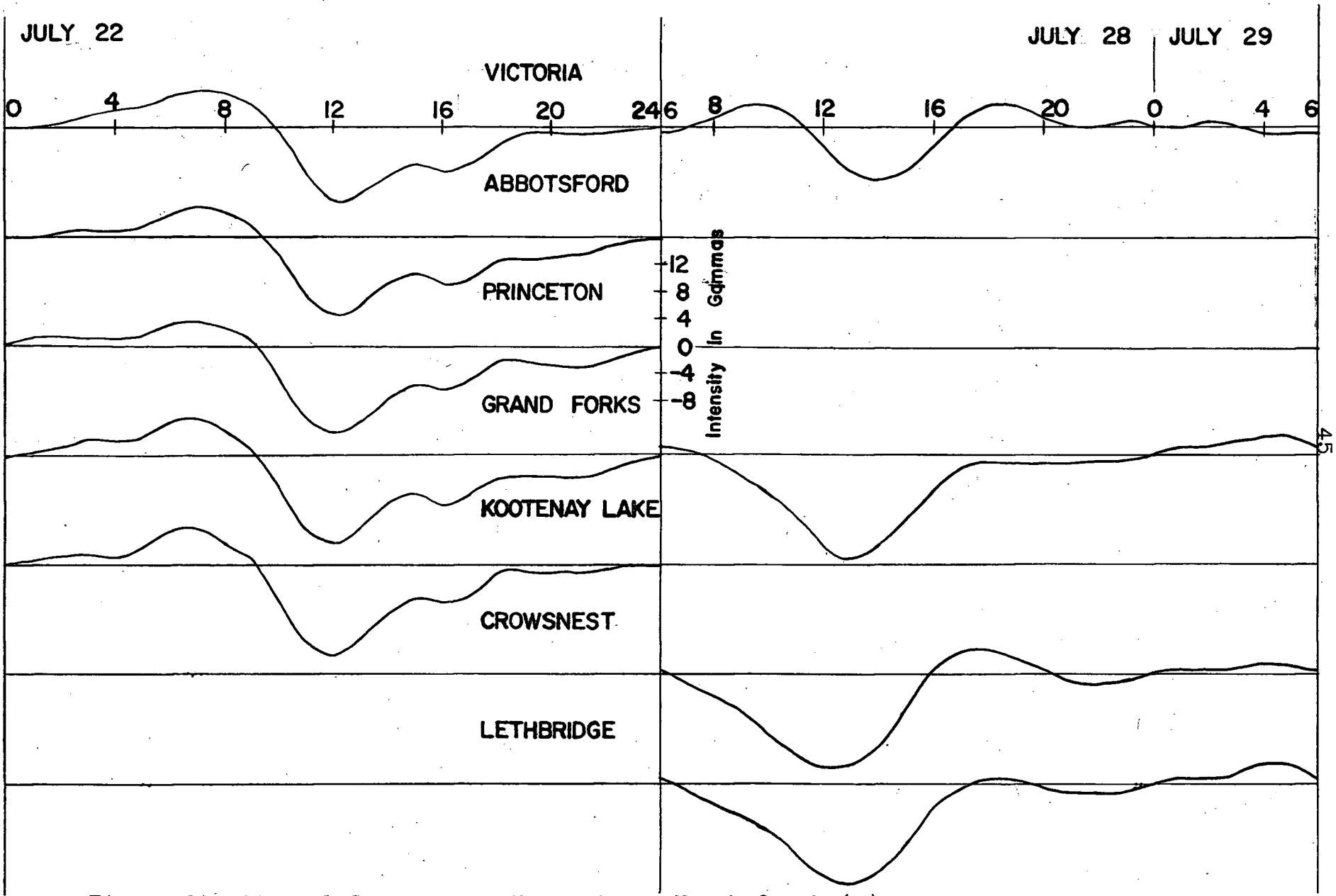

Figure 14. Diurnal Geomagnetic Variations, North-South (H) Component

only in the vertical component suggests a sharp vertical discontinuity (see model for a horizontally discontinuous structure). The skin depth for diurnal variations should be of the order of 400 km.

Some much smaller differences in the Z component are also indicated at the Abbotsford and Victoria stations.

2. Determination of the strike of conductivity inhomogeneities by extreme values

An attempt has been made to determine the direction, location and intensity of the nonhomogeneous induction that has produced the anomalous bay and magnetic storm features observed on the magnetograms for the 6 eastern stations. A comparison has been made between the extreme values of the normal field variations found at the Grand Forks station and those found at the anomalous stations. In section IV on induction analysis it was noted that for a two dimensional structure, only the incident field components perpendicular to the strike of the structure are effective in producing induced currents. The anomalous induced vertical field is then given by

$$\Delta Z_a = C \, \Delta F_n \cos(\alpha - \alpha_0)$$

where ΔF_n is the normal total horizontal field component

α is the angle the perpendicular to the strike of the conductivity inhomogeneity makes with magnetic north

$\alpha_0 = \tan^{-1} D/H$, the angle the normal horizontal field variation makes with magnetic north.

The following assumptions are necessary for the validity of this equation.

1. The anomalous zone is two dimensional. It should be noted that if the anomalous zone is roughly spherical α defines the direction from the station to the center of the zone.
2. The induced field is approximately in phase with the inducing field. This appears to be true for the periods used in this study.
3. The normal vertical field makes a negligible contribution to the induced currents. The amplitude of the normal vertical field is less than 20% of the normal horizontal so that the error introduced in the value of C by this assumption should be about 20%. In any case this assumption should introduce no error in the strike of the anomaly that is found.
4. The anomalous part of a disturbance may be approximately determined by subtracting the normal part as found at a "normal" station in the vicinity. Whitham[31] has made estimates of the differences to be expected between normal stations. From his results it appears that for a 200 km. east-west profile parallel to the auroral zone and during a period of only moderate magnetic activity the differences should be less than about 10% particularly when averaged over a number of features. To obtain another estimate of the possible error introduced here, an approximate strike of the inhomogeneous zone was found at the station (Lethbridge)

farthest away from the reference station (Grand Forks), and the difference in the horizontal components for the two stations, parallel to this strike determined. The component parallel to the strike should exhibit no anomalous induction effects. The difference averaged over 10 features was found to be 7.5% which is given as the limit of error for all stations. This technique might be used to scale the normal component values with respect to the reference station, but was not used here.

Extreme values of amplitude for a number of magnetogram features of different dominant harmonic periods and different azimuths of the magnetic vector were used to evaluate α and C using a least squares method. The amplitudes and periods were measured as shown in Figure 15. The choice of the points of measurement is somewhat arbitrary but is of less importance than the requirement that the same points be taken on each record. A statistical averaging should reduce any random errors. This method of measurement, in an approximate manner, eliminates both the longer period harmonics and instrumental drift.

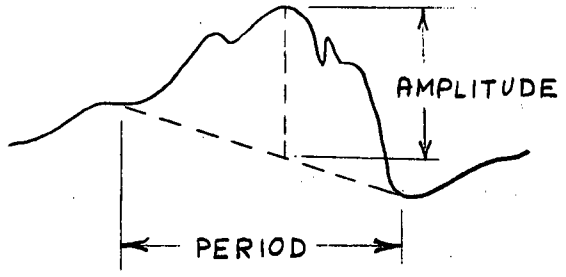

Figure 15. Measurement of the Extreme Value of a Feature on a Magnetogram.

In order to facilitate a least squares computation of α and C, it is convenient to utilize the data in the three component form given on the records[33]. The above equation is equivalent to

$$\Delta Z_a = A\Delta D_n + B\Delta H_n \quad \text{where} \quad \alpha_o = \tan^{-1} A/B$$

$$\text{and} \quad C = \sqrt{A^2 + B^2}$$

Dividing by ΔD_n or ΔH_n gives

$$\frac{\Delta Z_a}{\Delta D_n} = A + B\frac{\Delta H_n}{\Delta D_n} \quad \text{or} \quad \frac{\Delta Z_a}{\Delta H_n} = B + A\frac{\Delta D_n}{\Delta H_n}$$

These forms have been used in a least squares computation of A and B. They are preferable to the equation obtained by dividing by ΔZ_a which tends to be smaller than ΔD_n or ΔH_n and thus contains a larger percentage error.

As it is difficult to assign a specific period to any magnetogram feature C and α were determined for three ranges of periods, 7 to 20 min., 25 to 45 min., and 60 to 110 min. The computed values are given in Table 1. The strikes of the conductivity inhomogeneities are east-west for the Crescent Valley and Kootenay Lake stations and north-south for the eastern 4 stations. The consistent directions give some weight to the hypothesis that the zones are two dimensional. The recurrence of the same type of zone in the region of the eastern 4 stations indicates the anomalous fields are resulting from

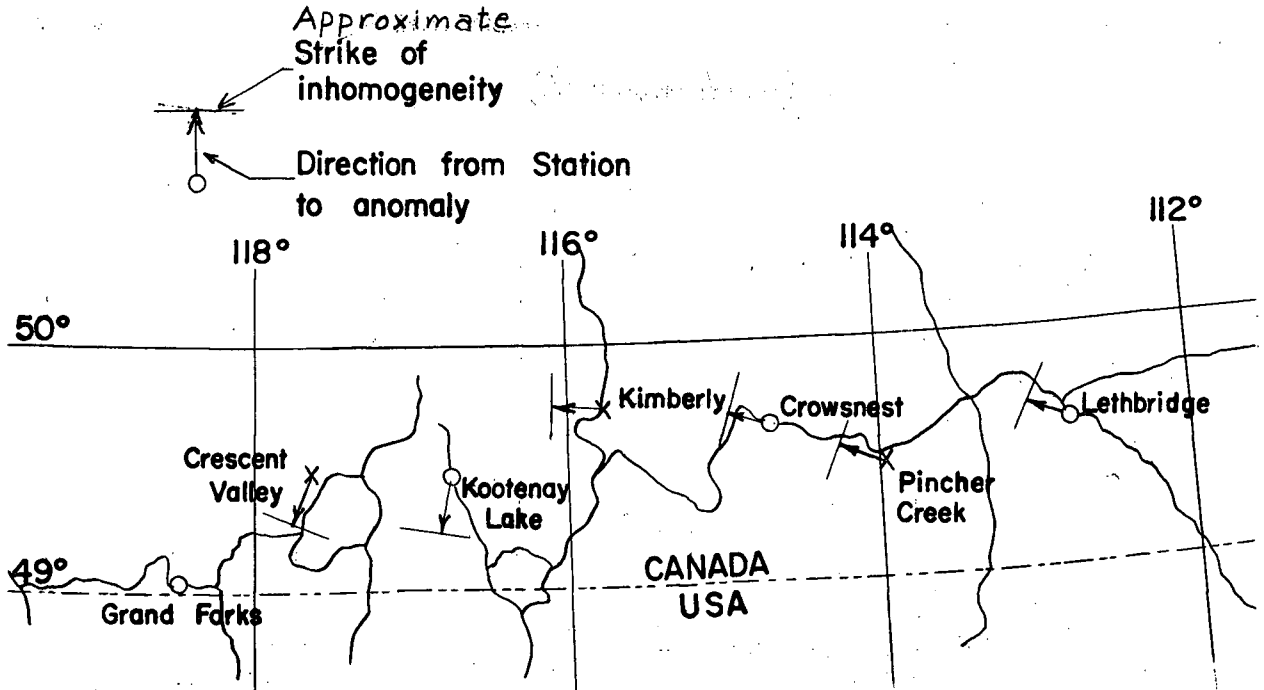

Figure 16. Strike of Conductivity Inhomogeneities From Least Squares Extreme Value Analysis.

Station		Period of Features 7 - 20 min.	25 - 45 min.	60 - 110 min.
Crescent Valley	β	109° ± 3° (Geog.)	106°30' ± 3°	121°30' ± 15°
	C	0.36 ± 0.04	0.31 ± 0.03	0.28 ± 0.06
Kootenay Lake	β	100°30' ± 3°	95° ± 3°	108°30' ± 12°
	C	0.67 ± 0.03	0.53 ± 0.03	0.50 ± 0.10
Kimberley	β	2°30' ± 4°	4° ± 4°	59°30' ± 30°
	C	0.30 ± 0.04	0.23 ± 0.03	0.27 ± 0.07
Crowsnest	β	26° ± 3°	22° ± 5°	69° ± 30°
	C	0.50 ± 0.03	0.40 ± 0.04	0.26 ± 0.07
Pincher Creek	β	23°30' ± 5°	42°30' ± 6°	5° ± 40°
	C	0.24 ± 0.04	0.30 ± 0.04	0.08 ± 0.10
Lethbridge	β	22° ± 8°	44° ± 5°	58°30' ± 15°
	C	0.25 ± 0.05	0.24 ± 0.04	0.28 ± 0.06

Table 1. Strike of Conductivity Inhomogeneities (β) and In Phase Induction Coefficients (C) From Extreme Value Analyses.

some recurrent structure such as a system of large north-south trending dikes of high conductivity.

3. Determination of induction coefficients as a function of frequency from a spectral analysis

A spectral analysis was performed on a bay type magnetic disturbance on August 4, 1963 at the Grand Forks and Kootenay Lake stations. Fourier components for frequencies from 0.008 to 0.200 cycles/min. were determined from readings at 2.5 min. intervals for a total length of 60 min. Simpson's interpolation rule was used on a digital computer. The spectral densities are given in Figures 17 and 18. A correlation between Z and H and an inverse correlation between D and H is quite clear at the Kootenay Lake station. No correlation is apparent at Grand Forks, 120 km. to the west. An attempt has been made to determine the in phase and out of phase induction coefficients at Kootenay Lake as a function of frequency from this data, using the spectral densities at Grand Forks as the normal field. This was unsuccessful, widely scattered values being obtained. It is apparent that either there is an appreciable difference between the external variations at the two stations or the spectral analysis was not sufficiently precise. It is suspected that the external field is not sufficiently uniform over the 120 km. distance to give accurate results.

4. Determination of the Location and size of an assumed infinite cylinder

In this section the conductivity inhomogeneities have been

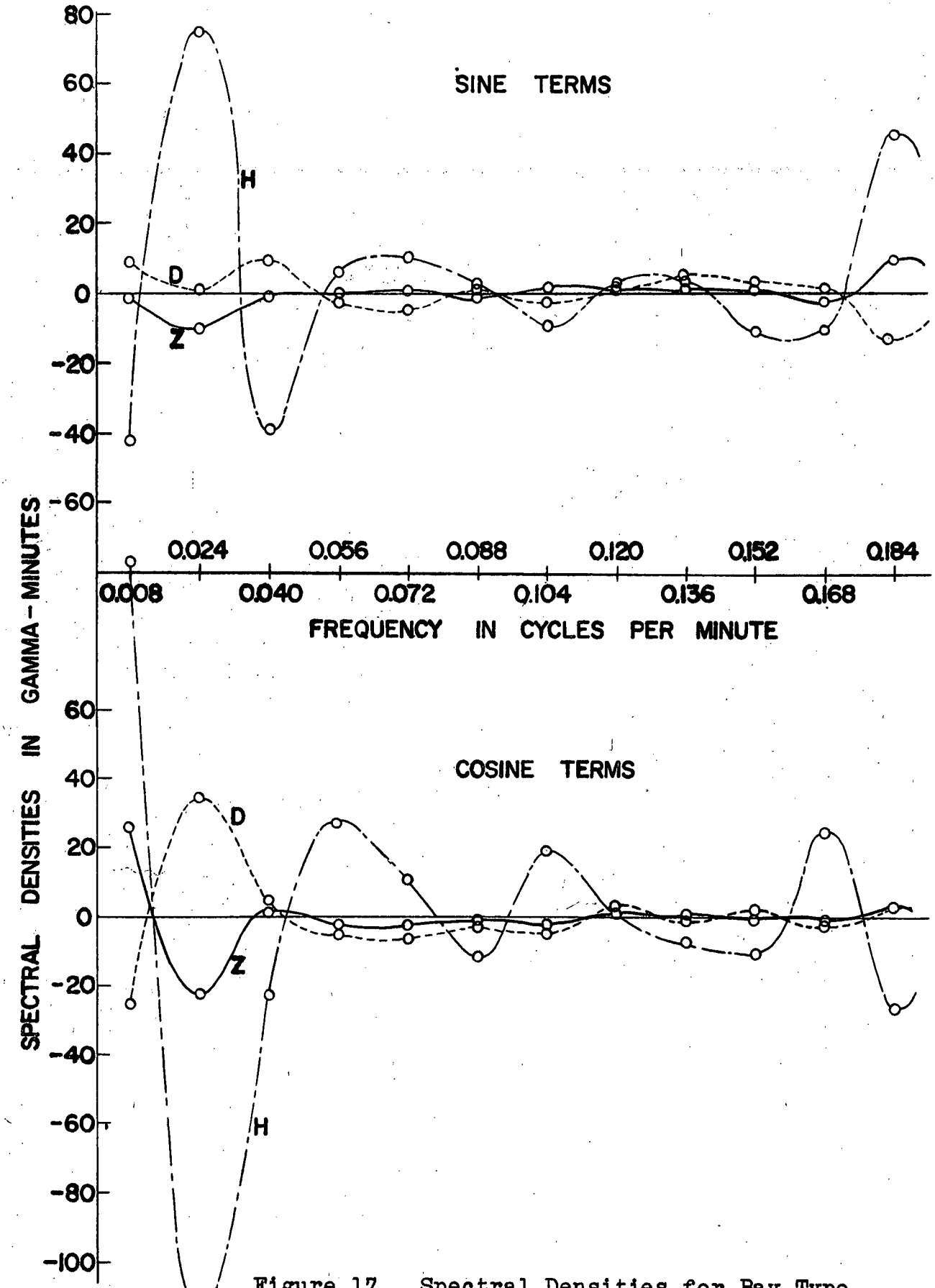

Figure 17. Spectral Densities for Bay Type Feature at Grand Forks on August 4, 1963.

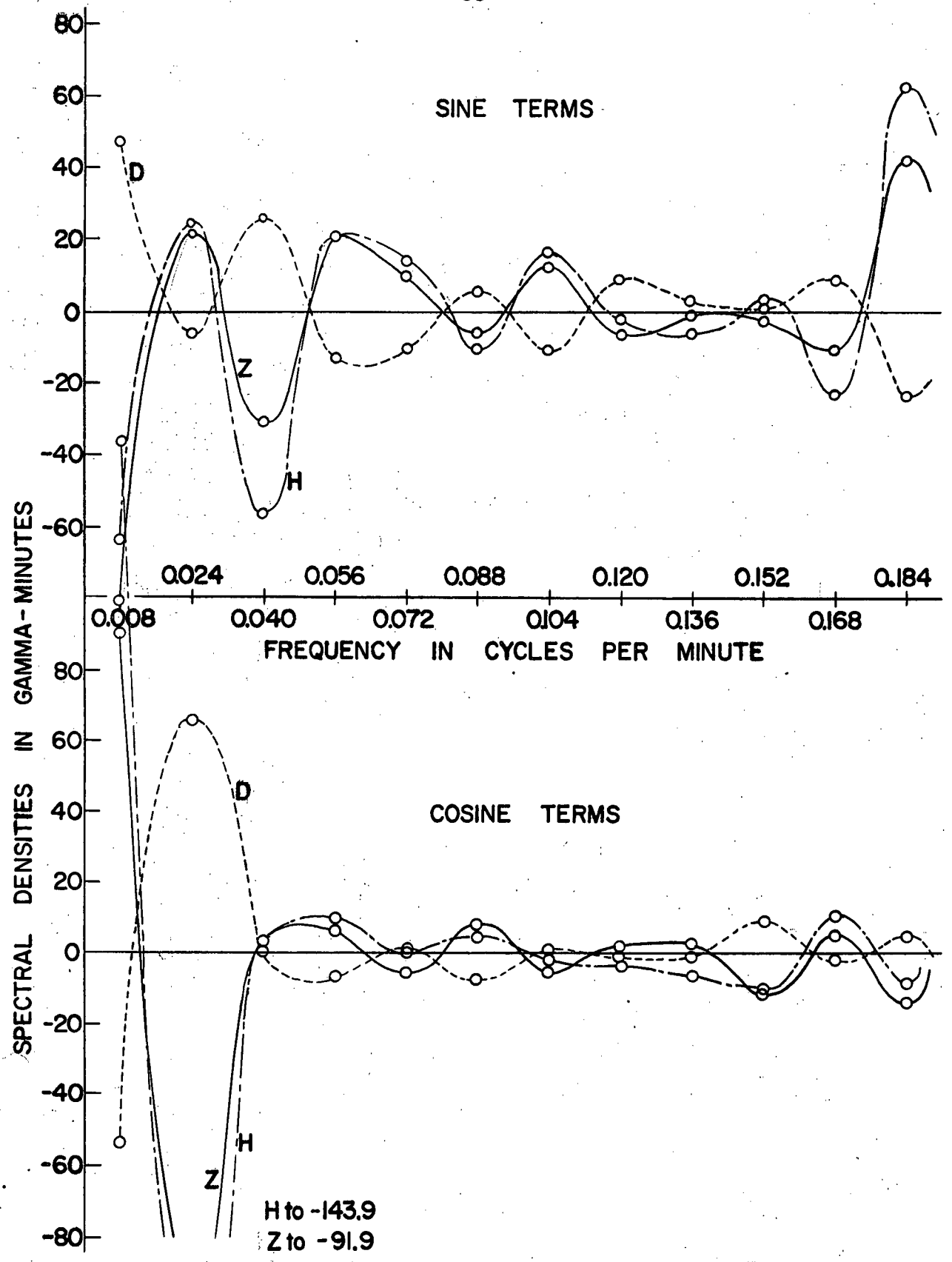

Fig. 18. Spectral Densities for Bay Type Feature at Kootenay Lake on August 4, 1963.

Station	Crescent Valley	Kootenay Lake	Kimberley
Dip Angle	$46^{\circ} \pm 5^{\circ}$	$51^{\circ} \pm 3^{\circ}$ 50° 6° (Spectral Analysis)	$71^{\circ} \pm 4^{\circ}$
Ratio of Radius to Distance	0.60 ± 0.06	0.82 ± 0.04 0.93 ± 0.20 (Spectral Analysis)	0.76 ± 0.07

Table 2. Cylinder Parameters for the Conductivity Inhomogeneities Observed from the Crescent Valley, Kootenay Lake and Kimberley Stations.

An examination of Table 2 shows that an assumed cylindrical zone south of Crescent Valley must extend almost to the surface while the computed cylinder to the south of the Kootenay Lake station extends to or slightly above the surface. An infinite cylinder thus can be only a very rough approximation to the shape of the high conductivity zone. If the assumed effectively infinite conductivity is reduced, a larger cylinder is required which would extend even further above the surface. A spherical body is even more difficult to reconcile with the observed data since a larger value of $\frac{\rho}{f}$ would be required for the same magnitudes of secondary induced fields. This adds weight to the conclusion that the anomalous zones may be closely approximated by two dimensional structures. Other idealized models such as a vertical discontinuity and a vertical dike have not been examined in this thesis because of the lack

of theoretical expressions for the secondary induced fields.

Finally, an estimate has been made of the conductivity of an assumed cylinder as seen from the Kootenay Lake station, using the spectral densities for the bay disturbance on August 4th. For a two dimensional structure, section IV gave the relations

$$Za_1 = A_1 Fn_1 + B_1 Zn_1 + A_2 Fn_2 + B_2 Zn_2$$

$$Za_2 = A_2 Fn_1 + B_2 Zn_1 + A_1 Fn_2 + B_1 Zn_2$$

Since the normal vertical field is small for this disturbance it has been neglected. Letting M and N represent the in phase and out of phase coefficients respectively, these equations become

$$Za_1 = M Fn_1 - N Fn_2$$

$$Za_2 = N Fn_1 + M Fn_2$$

Solving for M and N gives

$$M = \frac{Za_1 Fn_1 + Za_2 Fn_2}{Fn_1^2 + Fn_2^2}$$

$$N = -\frac{Za_1 Fn_2 + Za_2 Fn_1}{Fn_1^2 + Fn_2^2}$$

The axis of the hypothetical cylinder has been taken from the extreme value analysis, and the mean values of M and N evaluated for the period range from 25 to 125 min. These means are

$$M = 0.65 \pm 0.10$$

$$N = 0.22 \pm 0.05$$

$$M/N = 0.34 \pm 0.14$$

A very rough estimate of the conductivity of the anomalous zone may be found by applying these values to the computed curves for the in phase and out of phase components of induction in a cylinder. A value of approximately $1000/\rho^2$ e.m.u. is obtained where ρ is the radius of the cylinder in cm. A cylinder with a radius of 10 km. thus requires a conductivity of 10^{-9} e.m.u. (10^2 (ohm-m)$^{-1}$). A larger radius will give a correspondingly lower conductivity. At ρ = 30 km, $\sigma = 10^{-10}$ e.m.u. This is of the same order of magnitude as found by Whitham between Ellesmere Island and Greenland and by Schmucker for a region in Germany. If the normal conductivity is taken to be 10^{-14} e.m.u. (Srivastava et al[24]) the conductivity contrast is about a factor of 10^4.

5. Frequency dependence of the anomalous induced fields

The extreme value analysis shows a decrease in the ratio of induced to normal field components with increasing period of magnetic variation at all the anomalous stations. The spectral analysis was inconclusive. The shortest period range

studied by extreme values (7 - 20 min.), showed the largest intensity of induction. For a resistivity value given by Srivastava et al[24] for the southwestern Alberta region of about 1000 ohm - m. for depths from 2 - 8 km., a low resistivity surface layer and decreasing resistivity below 80 km., the skin depth for this period range is of the order of 100 to 150 km. The conductivity inhomogeneities may be expected to lie above this depth.

The anomalous diurnal variations should result from very much deeper inhomogeneities. For diurnal magnetic variations with a period of 12 hours, the skin depths for different Earth resistivities are given in Table 3.

(ohm - m)	d (skin depth in km.)
0.2	47
5	230
50	740
1000	3300

Table 3. Depth of Penetration of Diurnal Magnetic Variations.

VI. SUGGESTIONS FOR FUTURE STUDY

The first requirement for a more detailed study of the regions of inhomogeneous conductivity is a more closely spaced network of variograph stations. With the profile described in this thesis, only one or at most two stations are appreciably affected by the secondary fields from a single anomalous conductivity zone. The profile also appears to parallel the zone existing to the south of the Crescent Valley and Kootenay Lake stations.

With more detailed information it should be possible to make comparisons with the results for other idealized models such as a vertical discontinuity and a vertical dike. More theoretical work or laboratory model studies would also be necessary to determine the secondary induced fields to be expected for these and more complex structures.

With more detailed data it should also be possible to determine the internal and external parts to the observed field variations using the method outlined in the introduction. This would eliminate the problem encountered in determining the normal incident field from a non-anomalous station.

No correlation has been attempted with other techniques for investigating the deeper regions of the Earth's crust and upper mantle. Results from seismology, gravity, aeromagnetic, and geological studies should be considered.

The difference between the vertical component of the diurnal variations at Crowsnest and that at the remainder of the

stations is of major interest because of the depth of the structure it must reflect. A detailed profile across this area should be attempted.

One other concern that should be investigated is the difference in the intensity of the induced currents produced by different magnetic features at the same station, with the same period and approximately the same direction of the magnetic disturbance vector. The ratio of induced to inducing fields at Kootenay Lake varies from 20 to 80 percent on the same magnetogram. Such irregularities may invalidate any results from a spectral analysis of a single magnetogram feature.

VII. CONCLUSIONS

The study presented in this thesis suggests conductivity inhomogeneities of a varied nature extending from Crescent Valley, British Columbia to Lethbridge, Alberta. These have been detected by the anomalous secondary induced field components observed in the period range from 5 to 120 min. Using a least squares method the strike of the anomalous conductivity zones has been found at each anomalous station. This evaluation requires the assumption that all the zones are two dimensional. By making the additional assumption (which must be considered of doubtful validity) that the inhomogeneities approximate to highly conducting cylinders, estimates have been made of the position and size of the zones relative to the Crescent Valley, Kootenay Lake and Kimberley stations. An estimate of the conductivity contrast has also been made from the Kootenay Lake data. A difference has been detected between the vertical components of the diurnal geomagnetic variations at a site in the Rocky Mountains and those along the remainder of the profile. This should be of major interest.

APPENDIX I. LOCATION AND DETAILS OF THE STATIONS

Station	Type of Instrument	Geographic Long.	Geographic Lat.	Elev. (ft)	Total Field (gauss)	Duration of Observation
Westham Island	Fluxgate	124°49'W	49°5'N	10	0.5699	Jun 6 - Jul 11
Abbotsford	Askania	122°21'	49°1'	180	0.5735	Jun 15 - Jul 11
Hope	Fluxgate	121°29'	49°22'	130	0.5706	Jun 15 - Jul 11
Princeton	Askania	120°29'	49°28'	2300	0.5811	Jun 15 - Jul 12
Penticton Dom. Obs.	Fluxgate	119°38'	49°19'	1800	0.5777	Jun 15 - Aug 8
Grand Forks	Askania	118°28'	49°1'	1500	0.5777	Jun 14 - Aug 7
Crescent Valley	Fluxgate	117°35'	49°27'	2000	0.5811	Jun 20 - Aug 7
Kootenay Lake	Askania	116°45'	49°28'	1800	0.5830	Jun 15 - Aug 7
Kimberley	Fluxgate	115°47'	49°43'	3000	0.5849	Jul 14 - Aug 6
Crowsnest	Askania	114°45'	49°39'	4300	a) 0.5866 b) 0.5877	Jul 15 - Aug 6
Pincher Creek	Fluxgate	113°57'	49°29'	3790	0.5917	Jul 16 - Aug 6
Lethbridge	Askania	112°47'	49°39'	3000	0.5903	Jul 16 - Aug 5

APPENDIX II. TABLE OF EXTREME VALUES (Gammas)

PHASE I

Time	Period (Min.)	Westham			Abbotsford		
		D	Z	H	D	Z	H
June							
17 2150	25				25.7	9.2	-15.7
18 0640	65				34.3	-11.7	17.1
20 0030	55				-62.2	-19.5	-38.3
20 0440	55				-13.4	-8.9	-12.0
26 0100	60	-128.0	-59.0	-32.0	-130.0	-58.1	-33.9
26 1910	40	5.0	12.0	39.5	5.4	10.0	40.4
27 0130	50	52.5	15.0	-15.0	53.6	11.7	-15.4
28 0150	90	-41.5	-25.5	-14.0	-41.5	-25.0	0
30 1930	75	23.0	9.0	19.0	25.5	9.7	20.5
30 1715	8	-5.0	0	16.5	-5.4	2.2	16.8
July							
2 1715	10				-5.1	2.2	19.5
2 1740	7				-2.1	1.4	16.8
4 1800	35	15.5	-3.0	-54.0	15.3	-5.6	-58.1
4 2300	85	110.0	60.0	-28.0	113.9	53.4	-35.9
5 1750	20	-17.0	0	16.0	-11.5	2.5	20.2
6 0040	35	47.0	17.5	44.0	45.6	13.9	44.5
8 0010	40	-75.0	-19.0	-34.5	-76.9	-17.0	-34.2
8 0900	8	-8.0	0	9.0	-16.1	0.8	14.0
8 1355	7	-5.5	3.5	10.5	-6.7	1.7	8.9
8 1535	50	12.0	-6.0	-35.0	10.7	-3.9	-36.3
8 2100	40	68.5	14.5	-41.5	69.7	13.3	-43.8
8 2350	55	-58.0	-35.0	-26.5	-56.3	-26.4	-24.3

Time		Period (Min.)	Hope			Princeton		
			D	Z	H	D	Z	H
June								
17	2150	25	29.0	11.5	-14.5	32.5	17.0	-16.7
18	0640	65	34.0	-14.0	15.0	34.4	-18.5	20.8
20	0030	55	-66.0	-17.5	-42.5	-69.9	-22.9	-45.7
20	0440	55	-14.0	-7.0	-13.5	-25.0	-9.8	-14.3
26	0100	60	-134.0	-63.0	-40.5	-146.3	-70.6	-51.1
26	1910	40	5.0	6.5	41.5	5.4	10.4	45.7
27	0130	50	57.0	13.0	-19.0	61.9	14.6	-17.7
28	0150	90	-43.5	-26.5	-16.0	-46.0	-35.2	-6.8
30	1930	75	25.0	9.0	21.0	26.9	9.2	22.2
30	1715	8	-4.5	1.5	17.5	-6.2	0.3	17.1
July								
2	1715	10	0	1.5	15.0	-5.1	0.6	22.2
2	1740	7	-4.0	1.0	20.5	-2.4	0.3	17.1
4	1800	35	15.0	1.0	-58.0	15.6	-3.9	-64.1
4	2300	85	120.0	60.0	-26.5	129.7	66.5	-31.4
5	1750	20	-12.5	0	20.0	-12.9	1.2	22.8
6	0040	35	46.0	14.0	45.0	43.0	17.9	49.4
8	0010	40	-79.0	-23.5	-41.5	-83.7	-17.9	-45.4
8	0900	8	-15.5	0	12.5	-16.4	-1.2	15.3
8	1355	7	-8.5	-1.5	9.0	-7.5	0.6	10.2
8	1535	50	16.0	-11.0	-38.0	12.1	-5.1	-41.6
8	2100	40	75.0	8.0	44.0	80.2	16.4	-46.4
8	2350	55	-58.5	-31.0	-28.5	-61.9	-35.8	-28.0

Time		Period (Min.)	Penticton			Grand Forks		
			D	Z	H	D	Z	H
June								
17	2150	25	28.0	14.5	-15.0	38.2	15.6	-18.7
18	0640	65				30.4	-18.7	31.7
20	0030	55	-63.0	-21.0	-44.0	-66.6	-21.5	-48.2
20	0440	55	-24.0	-9.0	-13.5	-16.3	-10.0	-15.9
26	0100	60	-139.5	-70.5	-57.0	-150.0	-71.8	-75.1
26	1910	40	5.0	13.5	45.0	5.4	11.9	50.7
27	0130	50	65.0	15.5	-20.0	68.1	15.0	-19.7
28	0150	90	-41.5	-27.0	-18.5	-46.4	-31.5	-15.9
30	1930	75	21.5	10.0	20.5	30.4	6.9	24.7
30	1715	8	-5.0	3.0	17.5	-5.7	-0.9	19.0
July								
2	1715	10	-1.5	1.0	17.5	-4.6	-2.2	25.4
2	1740	7	-4.0	-2.0	22.0	-2.1	-1.6	19.3
4	1800	35						
4	2300	85	120.0	63.5	-30.0			
5	1750	20	-11.0	-1.5	23.0	-14.7	1.9	22.8
6	0040	35	35.0	16.0	42.0	33.5	15.6	57.1
8	0010	40	-80.5	-21.0	-47.5	-80.2	-13.4	-57.1
8	0900	8						
8	1355	7	-6.0	2.0	10.0	-7.7	0	9.8
8	1535	50	23.5	-9.0	-41.5	13.9	-5.9	-47.5
8	2100	40	78.0	17.5	-43.5	86.4	17.2	-41.2
8	2350	55				-59.3	-35.9	-30.1

Time		Period (Min.)	Crescent Valley			Kootenay Lake		
			D	Z	H	D	Z	H
June 17	2150	25						
18	0640	65				30.1	-34.9	33.4
20	0030	55				-78.7	-29.1	-55.4
20	0440	55				-12.7	-27.5	-17.4
26	0100	60	-153.5	-92.5	-102.5	-96.1	-131.6	-168.2
26	1910	40	5.5	22.5	59.5	8.9	30.9	55.7
27	0130	50	66.5	12.0	-34.0	85.0	-18.7	-26.1
28	0150	90	-46.0	-39.5	-27.0	-43.0	-54.2	-24.1
30	1930	75	31.0	11.0	25.0	32.6	12.2	26.4
30	1715	8	-6.5	4.5	24.0	-8.9	7.0	20.3
July 2	1715	10	0	6.5	28.0	-10.1	11.9	29.0
2	1740	7	-1.5	7.0	31.5	-7.3	11.6	23.2
4	1800	35	14.0	-15.0	-79.0	24.5	-24.2	-74.0
4	2300	85	145.0	76.5	-25.0	170.0	80.2	-31.3
5	1750	20	-14.0	7.5	27.5	-19.7	76.5	69.0
6	0040	35	35.0	51.5	67.5	18.2	14.4	26.1
8	0010	40	-80.5	-38.0	-61.0	-70.8	-43.1	-69.9
8	0900	8	-18.0	4.5	17.5	-24.8	11.3	17.7
8	1355	7	-9.0	-4.5	8.5	-10.1	6.1	10.4
8	1535	50	11.0	-15.0	-60.0	22.3	-24.5	-53.4
8	2100	40	88.0	14.0	-64.0	97.4	0	-45.0
8	2350	55	-61.5	-55.0	-23.0	-60.7	-73.4	-31.0

PHASE II

Time		Period (Min.)	Penticton			Grand Forks		
			D	Z	H	D	Z	H
July 17	0500	70				-92.9	-39.9	-74.5
17	2330	100				36.1	4.7	-20.6
18	0015	35	-20.0	-3.0	15.0	-23.2	-3.1	13.3
18	0415	45				-11.9	-6.2	-13.3
18	2030	30	0	3.0	11.5	-3.1	-0.6	15.2
19	0000	45				19.4	0	1.3
21	0300	10	-10.0	-6.0	-24.0	-10.3	-3.7	-28.5
22	0145	15	25.0	1.5	13.0	26.8	1.2	15.8
22	1045	7	7.5	3.0	-8.5	12.4	0	-12.4
22	2125	20	9.5	1.0	17.0	11.4	-1.9	18.4
22	2300	45	35.0	7.0	-24.0	41.8	5.9	-25.4
23	1400	15	20.5	0	12.0	20.6	-1.6	18.4
23	1850	35	89.0	14.0	46.0	87.2	13.1	63.4
24	0220	60				-63.0	-18.1	-29.2
24	1000	35	-22.5	-2.5	30.5	-28.4	-1.9	33.3
24	1025	45	21.5	2.0	-27.0	28.4	0.9	-28.5
24	1415	35	-2.5	4.5	32.5	-4.6	3.1	35.5
24	1435	35	2.0	-2.5	-26.0	1.0	0.6	-33.0
24	2155	25	105.0	6.0	45.0	107.8	5.9	55.8
25	0020	30	45.0	0	50.0	59.3	0.6	60.2
26	0115	80				-59.3	-35.6	-17.7

Time		Period (Min.)	Penticton			Grand Forks		
			D	Z	H	D	Z	H
July 27	0955	8				-10.3	0	6.6
27	1545	45				9.0	0	-30.4
30	1930	60				-7.7	0	22.2
30	2145	35	25.0	-5.0	-15.0	37.4	1.6	-15.9
31	0600	110				-87.7	-22.4	-29.2
31	1015	7				-20.1	0	13.9
31	1930	90				35.6	8.7	36.1
Aug. 1	1615	30				-12.9	3.1	34.2
1	2310	15	10.0	-1.0	-11.0	20.6	0	-15.2
2	1950	30	45.0	-2.5	-29.0	48.5	-1.6	-33.3
2	2150	40				49.0	6.2	-33.3
3	0825	8				-13.2	-0.3	9.2
3	1610	10				-2.3	-0.3	12.4
4	0920	7				8.8	-0.3	-8.9
4	1110	7				9.8	0.6	-9.5
4	1600	30				-8.3	3.1	28.5
5	0500	80				-42.3	-15.0	-33.6
5	1400	35				-9.8	12.5	21.6

Time		Period (Min.)	Crescent Valley			Kootenay Lake		
			D	Z	H	D	Z	H
July								
17	0500	70	-93.0	-60.0	-91.0	-97.9	-69.8	-86.4
17	2330	100	32.5	-2.5	-17.5	40.5	9.2	-23.2
18	0015	35	-21.0	3.0	21.0	-27.8	7.7	16.8
18	0415	45	-11.0	-13.0	-16.0	-8.1	-16.5	-16.8
18	2030	30	-4.0	5.0	17.5	-5.6	6.7	16.8
19	0000	45	19.5	-5.0	2.0	22.8	-6.7	1.2
21	0300	10	-15.0	-12.5	-29.0	-10.1	-21.4	-28.4
22	0145	15	25.0	5.0	11.5	25.8	7.3	12.2
22	1045	7	10.0	-3.5	-6.5	17.5	-8.6	-12.2
22	2125	20	10.5	5.0	21.0	10.1	6.1	19.7
22	2300	45	42.0	2.5	-25.5	48.1	-9.2	-26.1
23	1400	15	21.5	7.5	21.0	18.2	11.0	20.3
23	1850	35	98.5	28.5	65.5	87.3	30.6	65.3
24	0220	60	-63.0	-39.0	-46.0	-58.2	-45.3	-39.4
24	1000	35	-25.0	10.0	40.5	-38.0	22.6	43.5
24	1025	45	25.0	-13.0	-41.0	38.0	-21.1	-32.8
24	1415	35	1.5	12.5	45.0	-10.6	17.7	40.0
24	1435	35	-1.5	-11.5	-41.0	8.6	-17.7	-37.1
24	2155	25	106.0	9.0	54.5	114.1	5.8	51.6
25	0020	30	60.0	27.0	65.5	48.1	20.8	60.9
26	0115	80	-60.0	-53.0	-20.5	-57.2	-58.8	-20.9

Time		Period (Min.)	Crescent Valley			Kootenay Lake		
			D	Z	H	D	Z	H
July 27	0955	8	-11.0	3.5	9.0	-12.9	6.1	8.7
27	1545	45	0	-11.0	-40.0	11.4	-15.6	-32.5
30	1930	60	-9.0	6.0	25.0	-10.1	10.7	24.6
30	2145	35	35.5	-10.0	-23.5	47.6	-19.6	-22.6
31	0600	110	-88.5	-31.5	-30.0	-86.5	-33.7	-37.1
31	1015	7	-19.0	3.5	15.0	-25.0	11.9	14.5
31	1930	90	36.5	12.5	42.5	38.0	14.7	37.7
Aug. 1	1615	30	-9.0	14.0	40.0	-20.2	22.0	38.3
1	2310	15	20.5	-6.5	-20.5	25.3	-14.7	-17.4
2	1950	30	45.5	-11.0	-43.0	53.1	-22.0	-37.7
2	2150	40	50.0	-5.0	-40.0	57.2	-18.4	-33.4
3	0825	8	-13.5	3.5	9.5	-17.2	6.4	8.7
3	1610	10	1.5	3.5	13.5	-4.6	5.5	11.6
4	0920	7	8.0	-2.5	-8.5	11.1	-8.0	-11.9
4	1110	7	6.0	-4.5	-8.5	9.9	-6.7	-9.3
4	1600	30	-6.0	13.5	38.5	-15.2	20.2	34.8
5	0500	80	-44.5	-22.5	-44.0	-39.5	-23.9	-38.3
5	1400	35	-8.0	8.0	25.5	-13.2	12.9	24.9

Time		Period (Min.)	Kimberley			Crowsnest		
			D	Z	H	D	Z	H
July 17	0500	70	-124.0	-35.0	-85.0	-98.3	-39.1	-87.0
17	2330	100	45.0	-12.5	-22.5	38.3	15.6	-22.8
18	0015	35	-43.0	-13.5	24.0	-24.7	-15.3	13.3
18	0415	45	-7.5	-8.0	-16.0	-9.4	-6.2	-14.0
18	2030	30	-10.0	0	15.5	-6.4	-2.5	14.0
19	0000	45	33.5	4.5	4.0	21.7	7.4	4.2
21	0300	10	-24.0	-10.0	-26.0	-7.9	-10.2	-23.9
22	0145	15	30.0	9.0	12.0	21.7	10.8	12.6
22	1045	7	24.0	3.5	-13.5	14.8	9.9	-12.6
22	2125	20	18.0	3.0	21.0	7.9	1.4	16.8
22	2300	45	68.5	16.0	-26.0	48.9	19.2	-31.9
23	1400	15	26.5	5.5	22.0	17.3	2.8	21.4
23	1850	35	127.5	52.5	71.5			
24	0220	60	-66.0	-30.0	-42.0	-52.4	-24.9	-38.6
24	1000	35	-60.0	-11.5	37.0			
24	1025	45	57.0	8.5	-31.0			
24	1415	35	-25.0	0	42.0	-9.9	-5.6	35.1
24	1435	35	23.5	4.0	-35.0	8.4	6.2	-30.2
24	2155	25	154.5	42.0	52.0	103.7	45.0	53.7
25	0020	30	46.0	33.5	69.0	33.1	11.3	58.3
26	0115	80	51.0	61.0	-25.0	-61.3	-53.2	-26.0

Time		Period (Min.)	Kimberley			Crowsnest		
			D	Z	H	D	Z	H
July 27	0955	8	-22.5	-1.0	6.5	-11.4	-5.1	7.0
27	1545	45	23.5	0	-30.0	10.9	3.1	-28.0
30	1930	60	-15.0	-5.0	25.0	-8.6	-5.7	21.1
30	2145	35	78.5	13.0	-20.5	44.0	13.0	-21.0
31	0600	110	-95.0	-40.5	-37.0	-86.4	-23.2	-37.2
31	1015	7	-36.5	-4.5	13.5	-24.5	-8.5	12.6
31	1930	90	45.0	10.0	38.0	37.1	11.3	37.2
Aug. 1	1650	30	-35.5	-2.5	41.5	-18.3	0	31.6
	2310	15	40.5	6.5	-19.5	22.7	13.0	-17.6
2	1950	30	75.5	20.0	-39.5	48.4	21.5	-33.7
	2150	40	90.0	25.0	-36.0	52.9	30.0	-31.6
3	0825	8	-24.0	-3.5	10.5	-16.8	-7.4	9.1
	1610	10	-9.0	1.0	13.5	-4.7	-2.6	10.9
4	0920	7	17.0	1.5	-6.0	10.9	4.5	-6.7
	1110	7	19.5	1.5	-10.0	8.6	5.7	-9.8
	1600	30	-31.5	-1.5	36.0	-12.4	-5.7	30.2
5	0500	80	-38.0	-15.5	-41.5	-32.6	-15.8	-44.9
	1400	35	-20.0	-3.0	24.5	-13.3	-5.7	20.4

Time		Period (Min.)	Pincher Creek			Lethbridge		
			D	Z	H	D	Z	H
July 17	0500	70	-82.5	-34.0	-80.0	-95.4	-43.8	-89.2
17	2330	100	35.0	7.5	-20.0	39.4	14.1	-22.3
18	0015	35	-23.0	-13.0	11.5	-24.6	-12.5	9.6
18	0415	45	-9.0	-6.0	-15.0	-9.8	8.8	-15.8
18	2030	30	-6.0	-3.0	10.5	-3.9	-2.8	13.0
19	0000	45	20.0	4.5	6.5	20.2	2.5	6.2
21	0300	10	-13.0	-8.0	-19.0	-8.9	-9.4	-24.0
22	0145	15	24.0	6.5	11.5	19.2	8.1	11.0
22	1045	7	11.0	3.5	-9.5	12.1	6.9	-11.7
22	2125	20	8.5	-1.5	18.0	7.6	-2.5	14.4
22	2300	45				48.7	14.4	-20.2
23	1400	15	19.0	0	20.5	17.2	-2.5	23.7
23	1850	35	94.0	40.0	74.0	86.1	33.5	74.1
24	0220	60	-51.5	-25.0	-34.0	-55.6	-28.2	-39.1
24	1000	35	-29.0	-10.0	28.0	-29.5	-9.4	27.4
24	1025	45	26.0	11.0	-20.5	29.5	8.8	-20.6
24	1415	35				-5.9	-5.0	33.6
24	1435	35				3.4	5.0	-27.4
24	2155	25				93.0	30.4	52.8
25	0020	30				27.1	5.0	54.9
26	0115	80				-67.9	-61.3	-28.1

Time		Period (Min.)	Pincher Creek			Lethbridge		
			D	Z	H	D	Z	H
July								
27	0955	8				-9.6	2.8	5.5
27	1545	45				6.9	2.5	-30.2
30	1930	60				-7.4	-6.3	20.6
30	2145	35	43.5	15.0	-11.0	41.3	9.4	-13.0
31	0600	110	-72.0	-30.0	-35.0	-83.6	-25.0	-43.9
31	1015	7	-18.5	-4.0	10.5	-17.5	-3.4	15.1
31	1930	90	34.5	18.5	35.5	40.3	6.3	35.7
Aug.								
1	1650	30	-11.0	-5.5	25.0	-12.8	0	33.6
	2310	15	27.5	8.0	-14.0	22.1	7.5	-17.8
2	1950	30	46.0	16.0	-28.0	48.2	14.5	-30.9
	2150	40	50.0	26.0	-25.0	50.2	23.5	-27.4
3	0825	8	-14.0	-4.5	6.0	-14.3	-3.4	7.2
	1610	10	4.5	-1.0	11.0	-2.5	-2.5	10.6
4	0920	7	9.5	3.0	-4.0	7.9	1.9	-4.8
	1110	7	9.0	1.5	-7.5	5.4	2.8	-7.5
	1600	30	-10.0	-4.5	30.0	-8.4	-1.9	30.9
5	0500	80	-33.5	-14.5	-38.5	-35.9	-15.0	-41.2
	1400	35	-9.5	-5.5	18.5	-9.8	-5.6	19.9

APPENDIX III - MAGNETOGRAMS

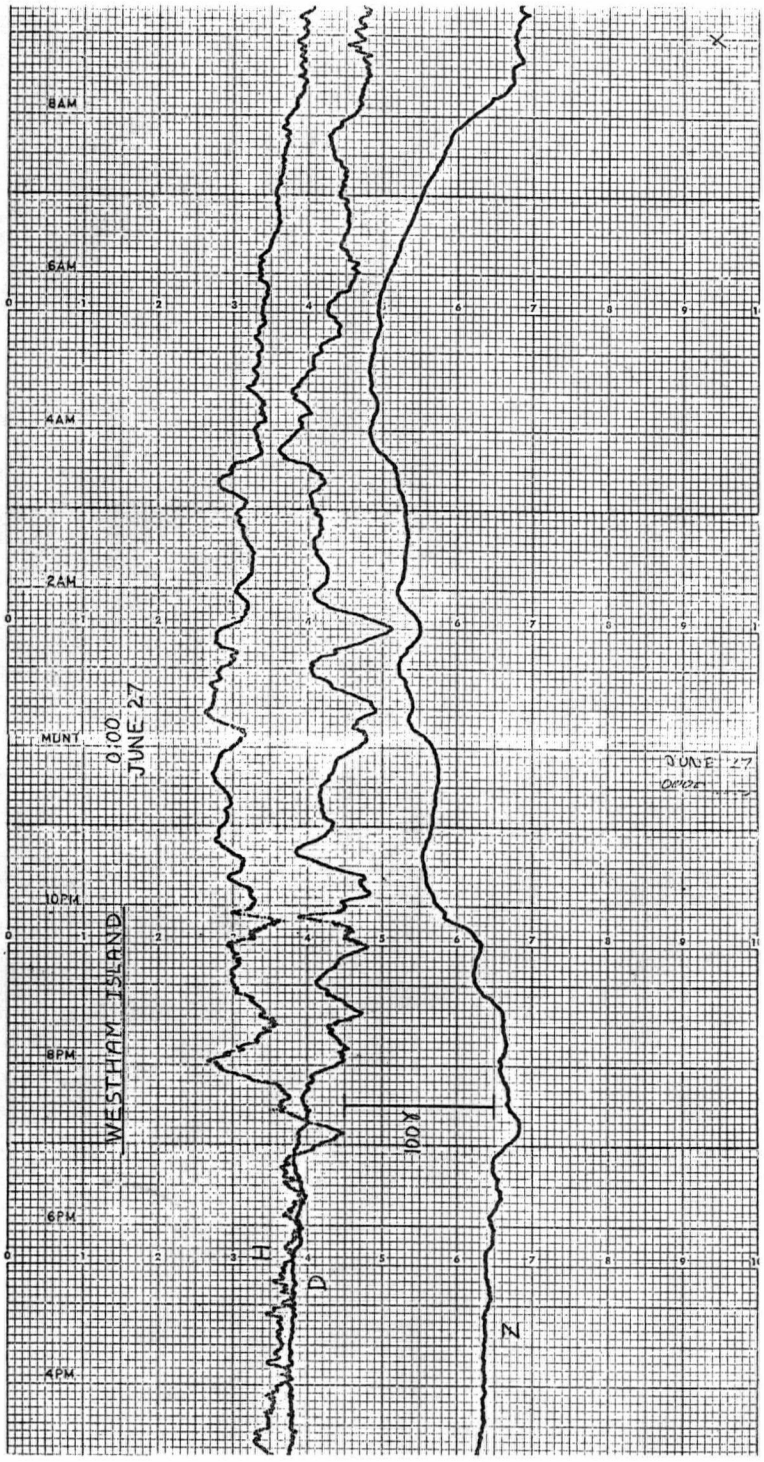

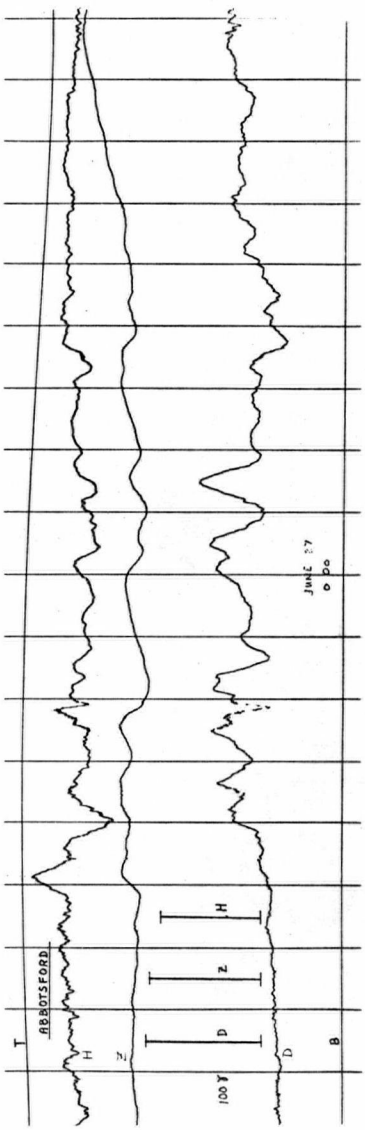

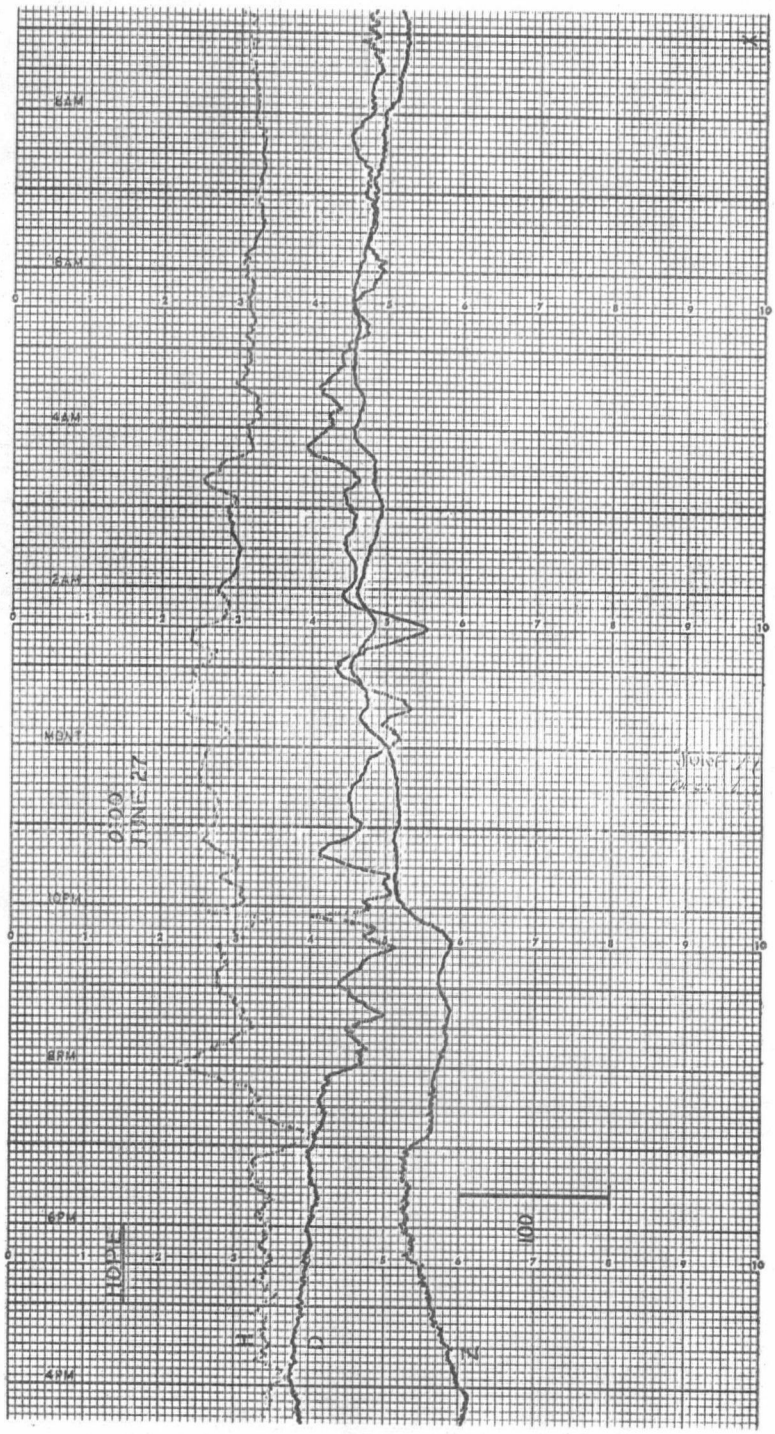
8AM
6AM
4AM
2AM
MDNT
10PM
8PM
6PM
4PM
GOOD
JUNE 27
H
D
Z
100

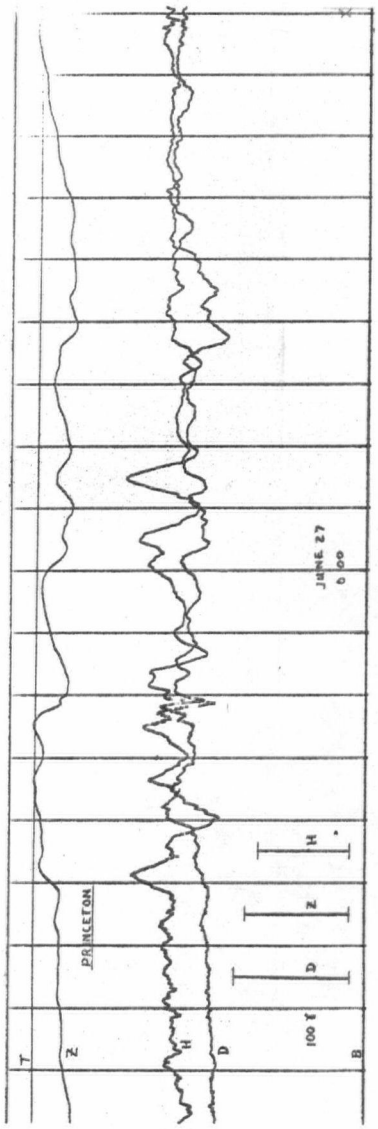
T
Z
H
D
PRINCETON
100 γ
JUNE 27
0 000

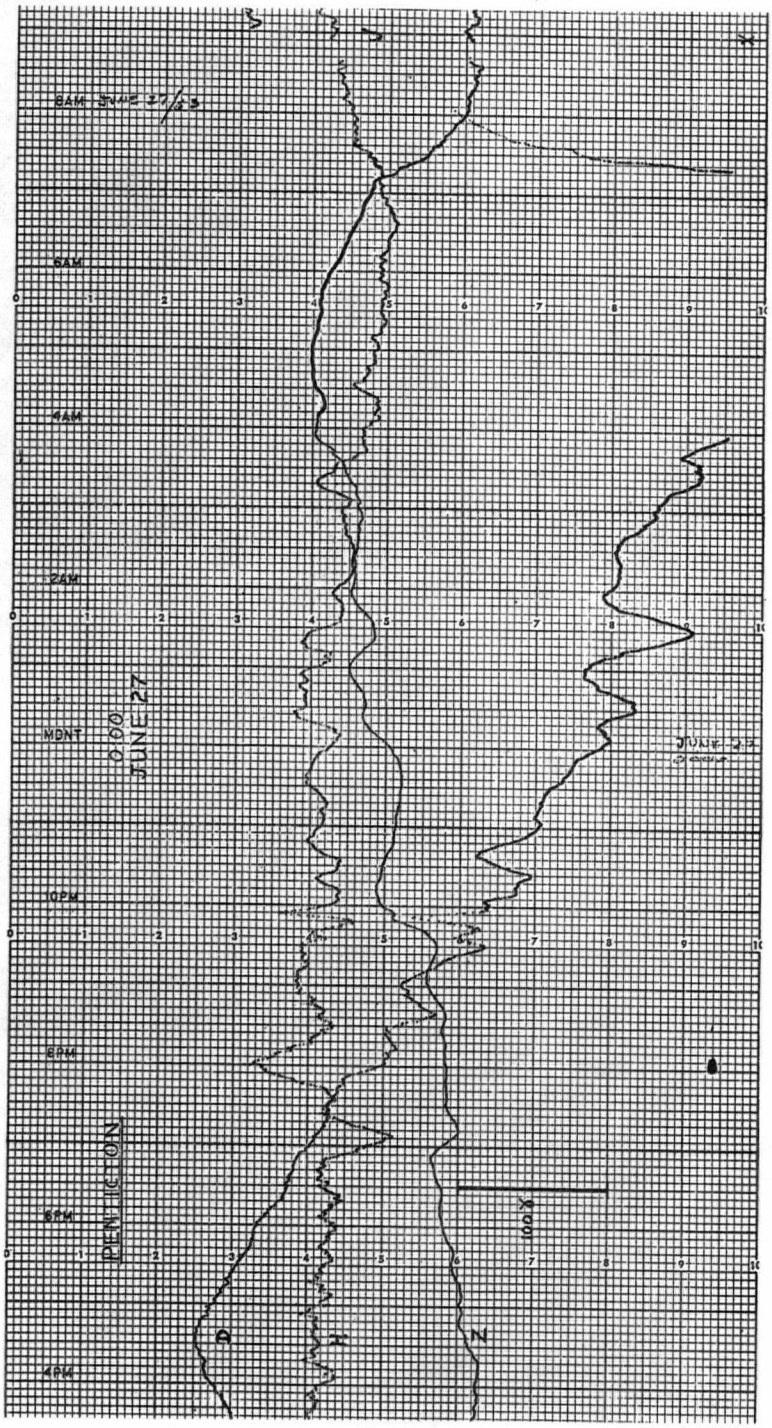
8AM JUNE 27/23
6AM
4AM
2AM
MDNT
10PM
8PM
6PM
4PM
0.00
JUNE 27
PENTICTON
100X
JUNE 27
H
N
D
R

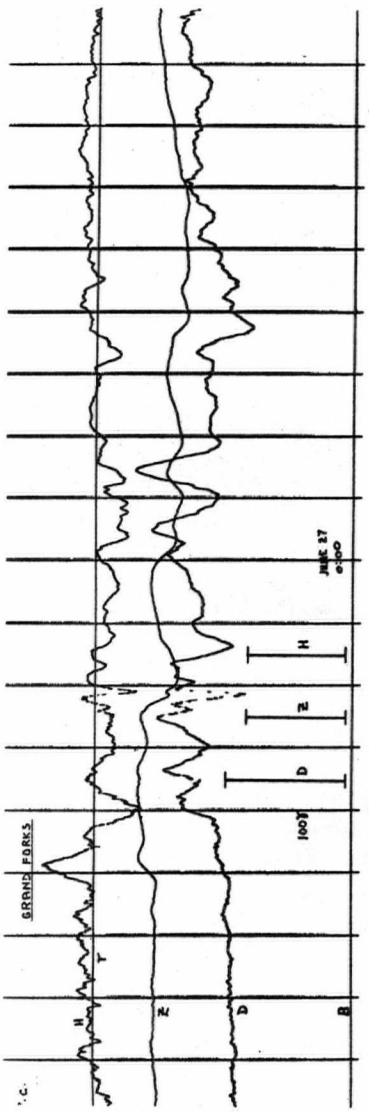
GRAND FORKS
100X
JUNE 27
0100
H
N
D
R

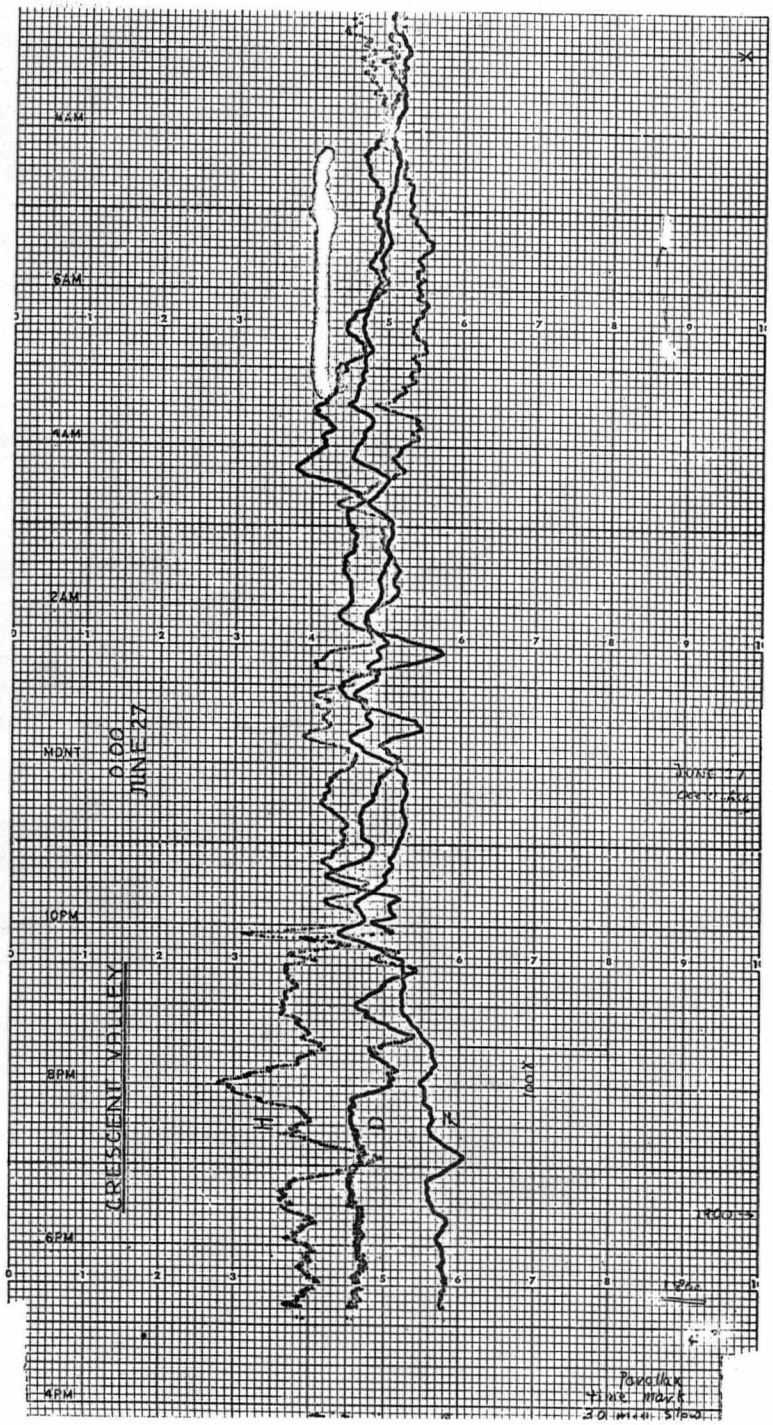
CRESCENT VALLEY
0.00
JUNE 27
MDNT
6AM
12AM
6PM
Parallax
Time mark

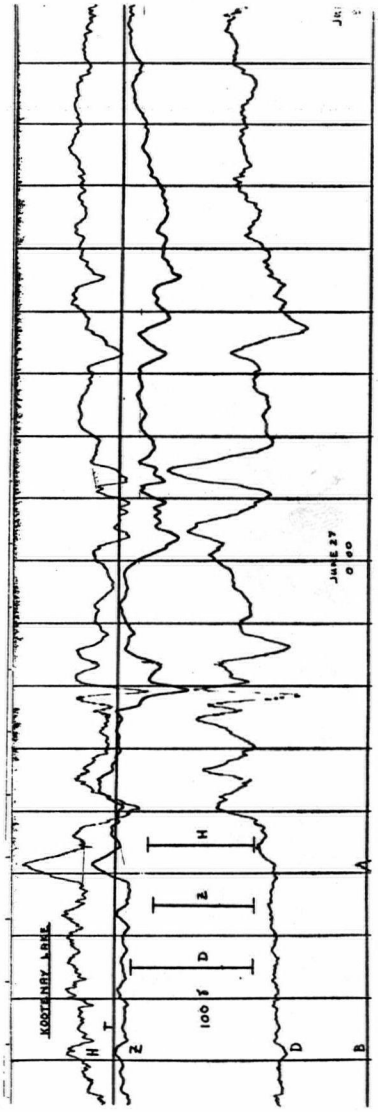
KOOTENAY ARRIE
JUNE 27
0.00

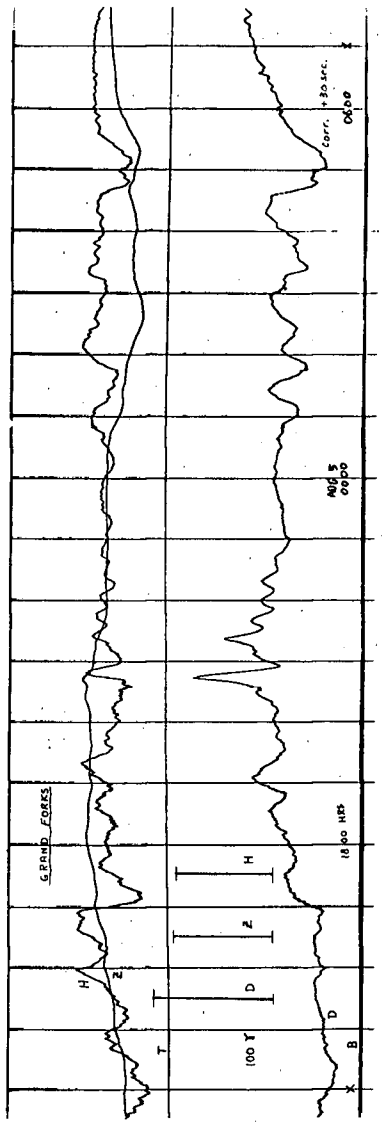
GRAND FORKS
H
Z
T
100 Y
D
Z
H
1800 HRS
D
B
AUG 5
0000
Corr. +30 sec.
0600

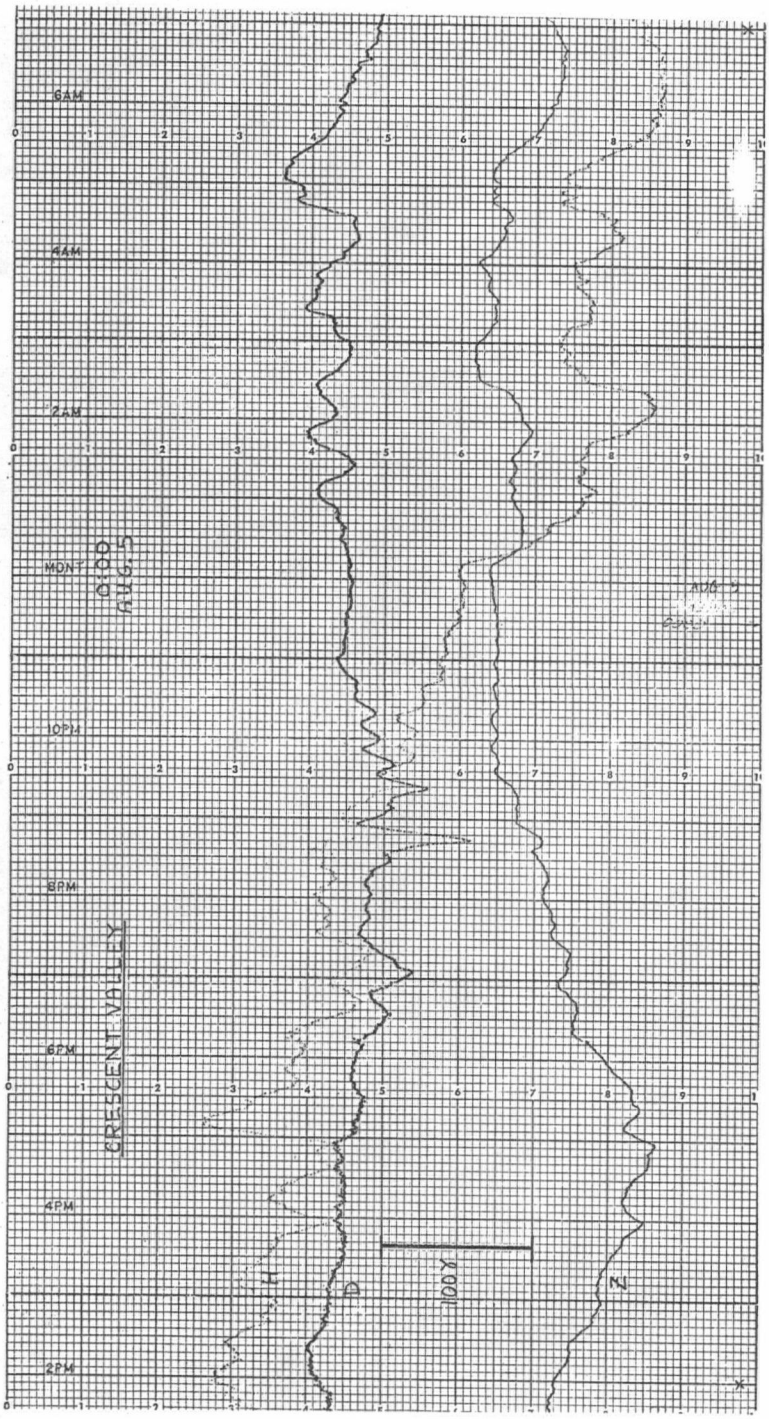
6AM
4AM
2AM
MDNT
10PM
8PM
6PM
4PM
2PM
CRESCENT VALLEY
AUG 5
0000
AUG 7
H
D
Z
100γ

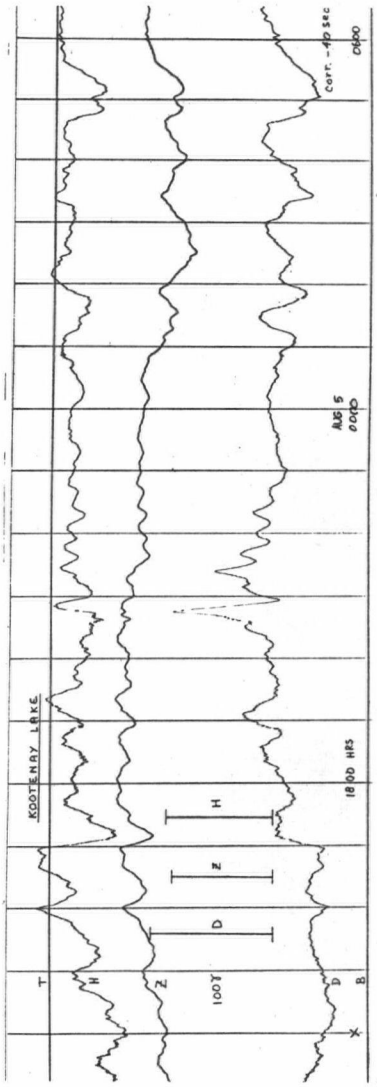
KOOTENAY LAKE
T
H
Z
D
100γ
AUG 5
0000
1800 HRS
Corr. -4p sec
0000

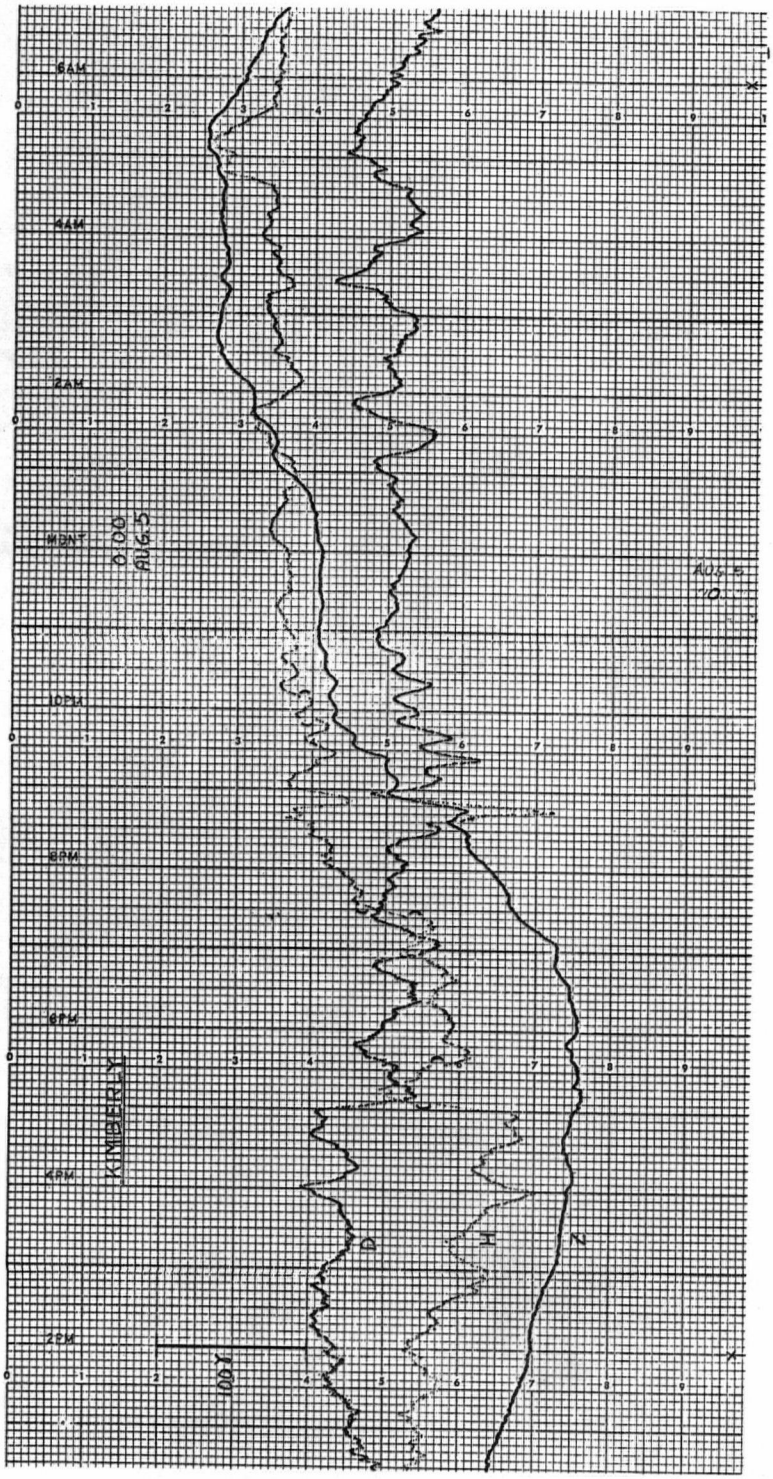
6AM
4AM
2AM
MIDNT
10PM
8PM
6PM
4PM
2PM
KIMBERLY
0.00
AUG 5
AUG 5
10
100Y
D
H
Z

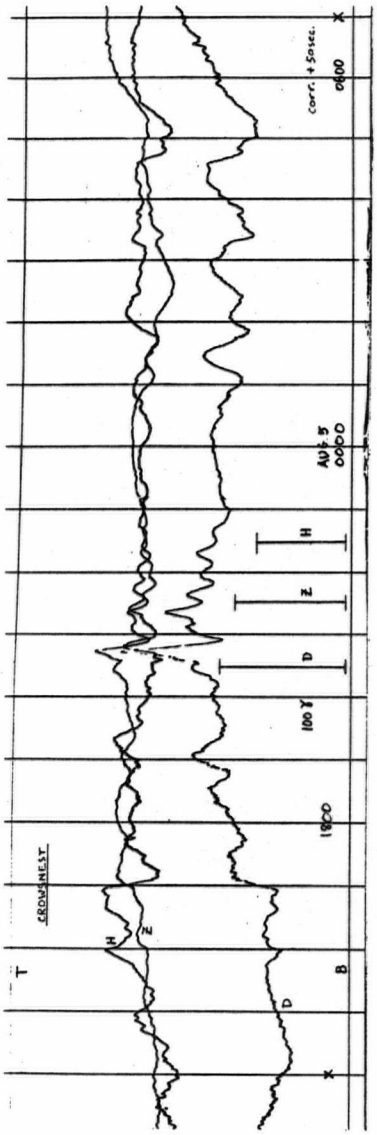
T
CROWSNEST
H
Z
D
X
B
1800
100Y
D
Z
H
AUG 5
0000
corr. + sasec.
0600
X

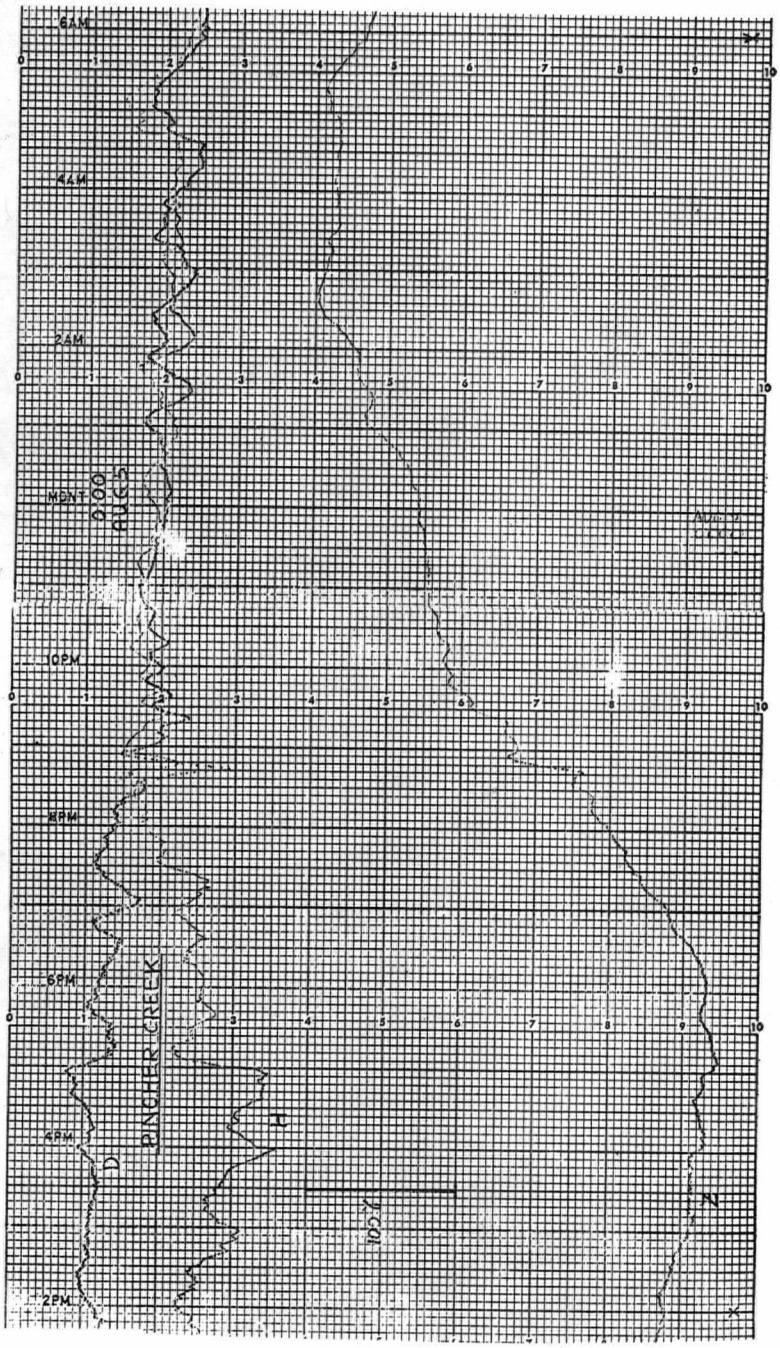
6AM
4AM
2AM
MDNT
10PM
8PM
6PM
4PM
2PM
AUG 5
9:00
PINCHER CREEK
100 CFS

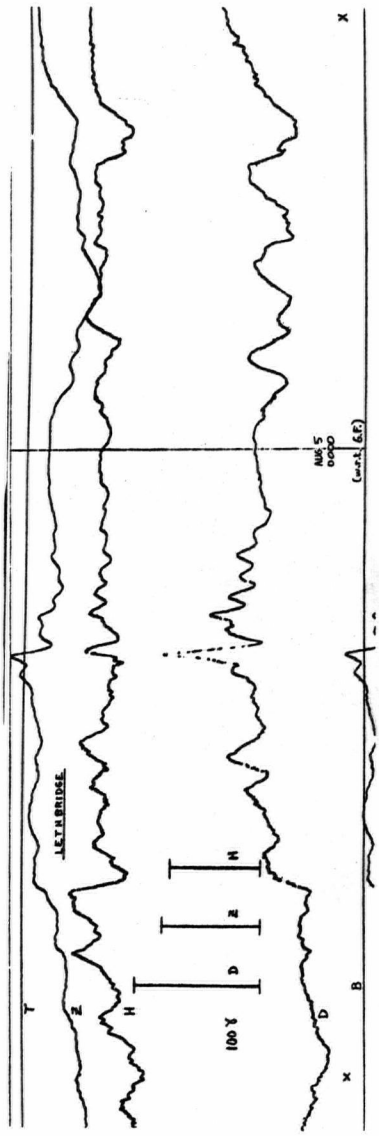
LETHBRIDGE
AUG 5
0000
100 Y

REFERENCES

1. Cagniard, L., Principals of the Magnetotelluric Method, a New Method of Geophysical Prospecting. Geophysics, 18, p 605, 1953.

2. Cantwell, T., Detection and Analysis of Low Frequency Magnetotelluric Signals. Ph.D. Thesis Massachusetts Institute of Technology, 1960.

3. Chapman, S., J. Bartels, Geomagnetism, v. 1 and 2, Oxford Press, 1940.

4. Christoffel, D., J. Jacobs, E. Jolley, J. Kinnear, J. Shand, The Fraser Delta Experiment of 1960. P.N.L. Lab. Rept. 61-5, D.R.B. Canada, 1961.

5. Coode, A., Electric and Magnetic Fields Associated With a Vertical Fault. M.Sc. Thesis, University of British Columbia, 1963.

6. d'Erceville, I., G. Kunetz, The Effect of a Fault on the Earth's Natural Electromagnetic Field. Geophysics 27, p 651, 1962.

7. Garland, G., T. Webster. J. Res. Nat. Bur. Stds., D, 64, p 405, 1960.

8. Holloway, J. (Jr.), Smoothing and Filtering of Time Series and Space Fields. Adv. in Geophy. 4, 1958.

9. Kertz, W., Leitungsfähiger Zylinder in Transversalen Magnetischen Wechselfeld. Erscheint in Gerlands Beit. Geophys. 69, 1, p 4, 1960.

10. Lahiri, B., A. Price, Electromagnetic Induction in Nonuniform Conductors, and the Determination of the Conductivity of the Earth from Terrestrial Magnetic Variations. Phil. Trans. Roy. Soc. Lond. A, 237, p 509, 1938.

11. Matsushita, S., Studies on Sudden Commencements of Geomagnetic Storms Using I.G.Y. Data from United States Stations. J. Geophys. Res., 65, 5, p 1423, 1960.

12. Niblett, E., C. Sayn-Wittgenstein, Variations of Electrical Conductivity with Depth by the Magneto-telluric Method. Geophysics, 35, p 998, 1960.

13. Parkinson, W., Directions of Rapid Geomagnetic Fluctuations. Geophy. J., 2, p 1, 1959.

14. Price, A., The Theory of Magnetotelluric Methods when the Source Field is Considered. J. Geophy. Res., 67, 5, p 1907, 1962.

15. Rankin, D., The Magnetotelluric Effect on a Dike. Geophysics 27, p 667, 1962.

16. Rikitake, T., Anomaly of Geomagnetic Variations in Japan. Geophy. J., 2, p 276, 1959.

17. Rikitake, T., A Possible Cause of Earth-Current Anisotropy. Bull. Earthquake Res. Inst., 40, p 685, 1962.

18. Rikitake, T., The Possibility of Detecting the Mantle Low Velocity Layer by Geomagnetic Deep Sounding. Bull. Earthquake Res. Inst., 40, p 495, 1962.

19. Rikitake, T., The Anomalous Behaviour of Geomagnetic Variations of Short Period in Japan and Its Relation to the Subterranean Structure. (10th Report). Bull. Earthquake Res. Inst., 40, p 693, 1962.

20. Rostoker, G., Low Frequency Variations in the Earth's Magnetic Field and Their Relation to the Conductivity of the Upper Mantle. M.A. Thesis, University of Toronto 1963.

21. Schmucker, U., Erdmagnetische Tiefensondierung in Deutschland 1957/59: Magnetogramme und Erste Auswertung. Abh. Akad. Wiss in Goettingen, Math-Phy. Kl. Beit. Inter. Geophy. Jahr Heft 5, 1959.

22. Schmucker, U., Annual Progress Report, Deep Anomalies in Electrical Conductivity. S.I.O. Ref. 61-13, Scripps Inst. of Oceanography.

23. Serson, P., An Electrical Recording Magnetometer. Can. J. Phys., 35, p 1387, 1957.

24. Srivastava, S., J. Douglas, S. Ward, The Application of the Magnetotelluric and Telluric Methods in Central Alberta. Geophysics, 28, 3, p 426, 1963.

25. Tozer, D., The Electrical Properties of the Earth's Interior. Phy and Chem. of the Earth, New York Pergammon Press, 3, p 414, 1959.

26. Wait, J., Some Solutions for Electromagnetic Problems Involving Spheroidal, Spherical and Cylindrical Bodies. J. of Res. N.B.S., 64B, 1 p 15, 1960.

27. Wait, J., A Conducting Sphere in a Time Varying Magnetic Field. Geophysics, 16, p 666, 1951.

28. Wait, J., On the Relation Between Telluric Currents and the Earth's Magnetic Field. Geophysics, 19, p 281, 1954.

29. Watanabe, T., On the Anomaly in the Vertical Magnetic Field Due to a Horizontally Discontinuous Structure. Personal Communication.

30. Weaver, J., A Note on the Vertical Fault Problem in Magnetotelluric Theory. Tech. Mem. 62-1, P.N.L., D.R.B. Canada, 1962.

31. Whitham, K., E. Niblett, The Diurnal Problem in Aeromagnetic Surveying. Geophysics, 26, p 211, 1961.

32. Whitham, K., F. Anderson, The Anomaly in Geomagnetic Variations at Alert in the Arctic Archipelago of Canada. Geoph. J., 7, 2, p 220, 1962.

33. Wiese, H., Geomagnetische Tiefentellurik Tiel II: Die Streichrichtung Der Untergrundstrukturen Des Elektrischen Widerstandes, Erschlossen Aus Geomagnetischen Variationen. Geofis. Pura E Applic., 52, p 83, 1962.

34. Erdmagnetische Tiefensondierung. Protokoll über das Symposion in Kassel am 1. und 2. Febr. 1962, Geschrieben in Institut für Geophysik und Meteorologie der Technischen Hochschule Braunschweig.